Response to Reviews

We thank both referees for their review and respond to them point by point below.

Referee #1

The manuscript entitled, "Size Dependent Chemical Ageing of Oleic Acid Aerosol under Dry and Humidified Conditions," by Al-Kinki et al. focuses assigning reaction products of the ozonolysis of oleic acid using ATOFMS. Exploring the chemical aging of organic particles relevant in the environment (or as proxy for structural similar systems) and developing new strategies for their quantitative analysis is certainly of fundamental interest. Given the complexity of atmospheric aerosol, laboratory experiments on confined systems are required for developing a better understanding of the complex processes occurring in airborne particles. Oleic acid (OL) + O3 has been extensively studied and there are key elements of the reaction mechanism that are still not understood and may involve the complex evolution of organic diffusion constants with extent of oxidation. The authors present a very detailed experimental description of the apparatus and have gone to impressive lengths to make the ATOFMS mass spectra, to C1 the extent possible, quantitative. The mass spectral assignments are plausible and the authors present, in most cases, reasonable mechanistic routes for the formation of the high molecular weight products. Since this reaction has been extensively studied, and is a subject of an extensive data evaluation and review paper by Zahardis and Petrucci, the expectation is elevated for any new paper reporting and interpreting results on this reaction in light of the extensive existing literature.

The main weakness of the work, which should be addressed by the authors, is the absence of interpreting the observed products within a full kinetic framework (especially in light of previous literature) as detailed below.

1. The connection between the SMPS measurements of particle size (dry and wet) are disconnected from the main theme of the paper which is chemical composition via ATOFMS. The ATOFMS instrument sizes by aerodynamic flight time, so it is not clear what additional information is provided by the SMPS? The authors observed the expected decrease is size previously observed in many other studies. The difference between dry and wet size reduction is insignificant statistically. Therefore, the authors should either better justify the inclusion of the SMPS data and discussion for the main focus of the paper or remove it for brevity.

<u>Response</u>
We believe that the SMPS data provides useful information. Whilst the results were statistically insignificant, there is a suggestion in the data that water might affect the oxidation mechanism "The fact that less mass loss was observed under humidified conditions than under dry conditions (although the difference was statistically insignificant), suggests that the presence of water might have an effect on the oxidation mechanism." The reviewer is correct that the SMPS data is not the main focus of the paper. However, we think it is better placed in the main text rather than the supplementary information.

2. Much of the mechanistic discussion is predicated on the size dependent concentrations shown in Fig. 7 and 8, which doesn't adequately normalize for extent of reaction (# of reactive collisions), since at a single ozone exposure the concentration (even without secondary chemistry) of OL will be size dependent. So any mechanistic conclusions based upon particle size drawn from Fig. 7 and 8 is ambiguous at best. For example, page 23 line 2 it is not unsurprising that larger particles contain more unreacted OL than smaller particles; this is exactly what you would expect kinetically given the difference in the number of OL molecules vs. size and the differences in surface area vs. size. So this observation alone is not sufficient to conclude that limited OL or O3 diffusivity is the cause. This conclusion originally reported by

Smith 2002 was drawn only after the full particle size kinetics ([OL] vs. ozone exposure) was measured and C2 reactive uptake coefficients where computed and were then found to be size dependent. Later on page 23 line 13-14 the authors conclude that the molar ratio of O3:OL is smaller for larger particles. . . .in order to explain larger OL for bigger particles in Fig. 7 and 8. Again I don't see how this works since at a fixed ozone concentration larger particles (due to S/V ratio) will always have a less extent of reaction than smaller particles. Furthermore, the authors state that ozone is not appreciably diminished inside their reactor when particles are present. So it is not clear how this small molar ratio of O3:OL works then. Won't the Henry's law constant imply that the [O3] is independent of size? Again on page 24 line 15-16 there is a statement about lower concentration of OL in smaller particles. . . but again this could just arise from a larger extent of reaction for smaller particle than larger ones at a single ozone concentration. It may well be the case that different chemistries are operative in larger particles (secondary chemistry) but such a comparison needs to be done by first eliminating the trivial size dependence due to kinetics. Furthermore, I don't observe any consistent monotonic trend in OL (or ON, NN, HMW) vs. size for example. The authors should address this. The quantity of OL (fig. 7 and 8) oscillates as a function of size, suggesting simply measurement error or uncertainty rather than a robust trend in secondary chemistry/diffusion as a function of size. Some error analysis needs to be shown and included in Fig. 7 and 8.

Response
On reanalysis of the data we realized we had made a small error in the initial analysis used to average the size resolved data. We have now replaced the old analysis data with the reanalysed data in the manuscript. The reanalysis of the data has not changed the conclusions from the paper but does smooth the trend in the size resolved data. In particular, the major observation of high molecular weight products resulting from the wet oxidation but significantly less in the dry oxidation remains the same. Figures 7 and 8 have been adapted.

3. Smith et al. 2002 observe that the uptake coefficient decreases with increasing size. How is this observation reconciled with the present study in which formation of HMW species is observed in large particles, since the mechanisms presented for HMW formation involve the consumption of more than one OL molecule (i.e. secondary chemistry, see R1 and Scheme 2). Thus it would seem from the present results, that larger effective uptakes are expected for larger sized particles (more secondary chemistry since there are additional sinks for OL, rather than just O3) which would be exactly the opposite trend observed by Smith et al. Size dependent kinetic measurements would offer a tangible way to connect the formation of HMW with previous size dependent uptake coefficient measurements of Smith et al.

Response
The Lovett et al. paper (2005) which comes from the same research group as Smith et al. (2002) shows that the kinetics of oleic acid ozonolysis is dependent on particle size since it is a surface limited reaction. However, the uptake coefficient remains the same regardless of size. We observe the same result as Lovett et al. (2005), see response to point 4.

4. It is not clear to me why, given the experimental setup (ATOMS, SMPS, AFT) why the authors did not measure the OL decay kinetics and product formation kinetics vs. Ozone exposure. This would have addressed #2 above as well as provided needed evidence for some of the proposed reaction mechanisms described throughout the manuscript. This would be entirely new by providing a potential new connection between reactive uptake, particle size, HMW, and diffusive limitations. Furthermore, there should be distinctive kinetic signatures based upon the proposed reaction mechanism. For example, the formation of NN via the decomposition of the primary ozonide (route 1 scheme 2) would be expected to have a different kinetic evolution than NN formed via the reaction of CI1 addition to the OL double bond and subsequent decomposition (as shown in scheme 2). Since the former NN pathway only involves

consumption of 1 OL in contrast to the latter which requires for its formation the consumption of 2 OL. This is also true for example in Scheme 3, where AA is formed by CI1 + ON but also could be formed by isomerization CI1 directly.

Response
The aim of this research was not to investigate the kinetics of oleic acid ozonolysis in detail. However, subsequent to the review we have reinvestigated our data sets and we are able to provide several pieces of kinetic information which will be of interest to the reviewer and reader.

We have generated a dataset investigating the kinetics of the ozonolysis of a near-monodisperse sized ensemble of oleic acid particles in the size range of 0.4-0.5 μm with a mean diameter of 0.48 μm. Through the use of 3 different sized aerosol flow tubes (AFT) the interaction time between ozone and oleic acid particles could be obtained at 20, 50 and 135 s. The longest time was the same as that used in the product distribution study shown in Figures 7 and 8. In the absence of O_3 the effective interaction time is zero. We observed that the concentration of oleic acid was negligible at the longest interaction time (135 s) and hence the kinetics could only be followed in the time range of 0-50 s. The kinetics of the loss of OL was measured under both dry (0.5% RH) and humidified (65% RH) conditions. No significant difference was observed in dry and wet kinetics which is expected since oleic acid is only marginally hygroscopic and any water that is available will very likely partition to the hygroscopic region of the molecule around the carboxylic acid functional group and not the lipophilic C=C double bond where the ozonolysis occurs. Since the wet and dry runs were very similar, data from both runs were combined into a single dataset to increase the data points available for analysis. The measured data show a linear relationship between the plot of $\ln\{S(OL)/S(OL_0)\}$ versus interaction time, where $S(OL)$ is the oleic acid signal, as shown in figure 9 below. This is consistent with surface limited reaction, as described by Case 3 kinetics initially proposed by Hearn et al. (2005). Using the same approach as Hearn et al. (2005), using the Case 3 kinetics approach, to derive gamma uptake coefficients (γ), we obtain $\gamma = 5.6\pm0.2 \times 10^{-4}$ which is similar to previous measurements of γ, e.g. Hearn and Smith (2004), Moise and Rudich (2002), Hearn et al (2005), Thornberry and Abbatt (2004), Ziemann (2005), Knopf et al. (2005).

In addition to the oleic acid reactive decay kinetics, we also observed the time dependent formation of the four major first generation reaction products nonanoic acid (NA), azelaic acid (AA), nonanal (NN) and oxononanoic acid (ON), see Figure 10. The high molecular weight (HMW) products were not observable in these experimental runs; this is consistent with the low levels observed in figures 7 and 8 in the 0.3-0.5 μm size bin. It is noted that low levels of HMW products were observed in the product distribution study but longer averaging times were used. It is clear that whilst the kinetics of oleic acid loss is very similar under both dry and humidified conditions, there are obvious differences in the formation kinetics of the four major first generation reaction products. In particular, under dry conditions the reaction products form more promptly, and once formed stay at relatively similar concentrations. Under humidified conditions the formation of the peak concentration of the products is slower but also their subsequent loss is more substantial. The kinetic data does not provide any definitive mechanistic understanding. However, these results are consistent with the hypothesis that water can act as a reactant with the CI thereby reducing the amount of secondary chemistry observed between OL and the primary reaction products, hence the more stable product distribution after the initial ozonolysis step.

A new section (starting on P27) now details the kinetics of oleic acid ozonolysis.
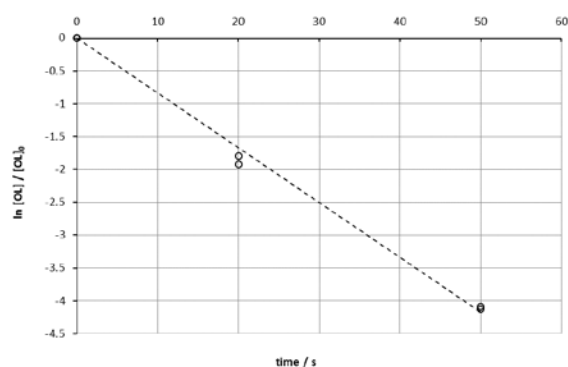
Figures

Figure 9. Reactive decay of oleic acid as a function of time for particles in the size range 0.4-0.5 μm (mean diameter = 0.48 μm). Black circles = measurements, dashed line = linear fit with intercept set to zero. Both the dry and wet kinetic data has been combined in this plot.
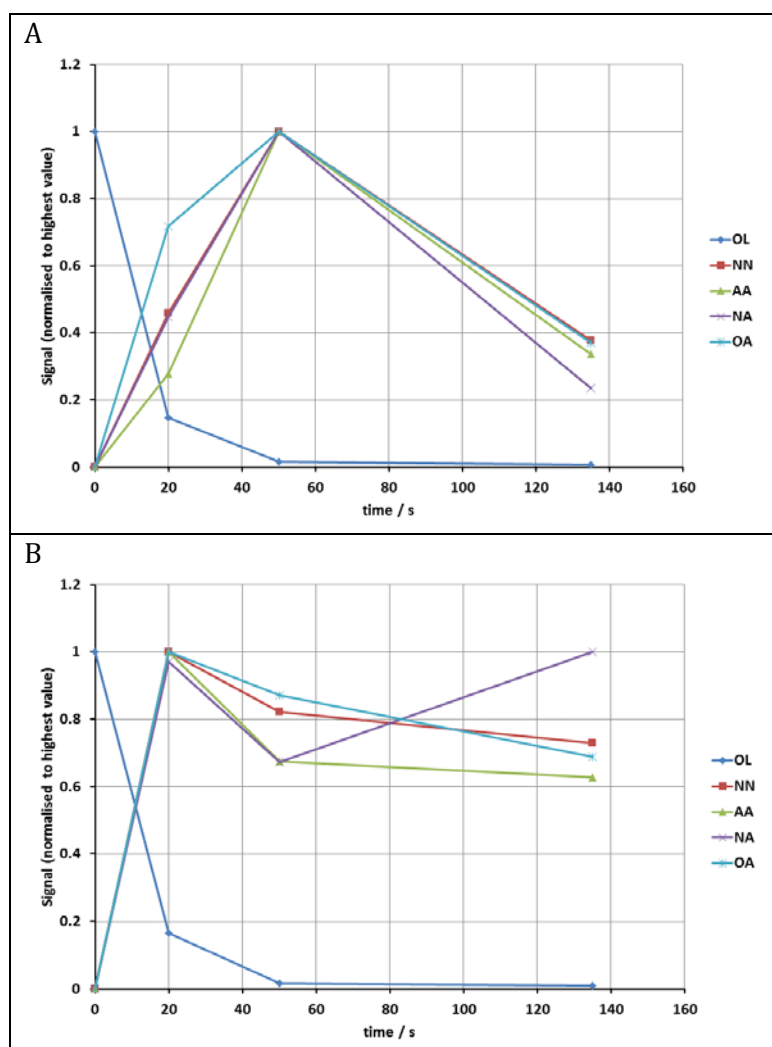

Figure 10. Time dependent signals of oleic acid and the four major first generation ozonolysis products. Graph A was obtained under dry conditions (RH = 0.5%) and B was obtained under wet conditions (RH = 65%). To aid ease of comparison of the different time series, the signals for all investigated species have been normalized relative to the peak signal achieved by the species investigated.

In summary, the logical arguments about mechanisms based upon difference in OL concentration (and other products) in small and large particles does not necessarily follow, given the way the experiments were performed (all sized measured at a single ozone concentration) and the lack of full kinetic measurements ([OL] vs. Ozone exposure) is needed to compare the same extent of reaction for each particle size. Although it is clear the authors observe some new HMW species whose identification is important for the community, the manuscript needs to be significantly revised for clarity, and further kinetic measurements might be required.

Response
We believe our responses to the major points raised by reviewer 1 answer this last paragraph.

Minor Comments:
1. The split axis, while certainly convenient, makes it very difficult for the reader to ascertain the true relative intensities of the peaks in the mass spectra shown in Figs. 5 and 6. Please reformat these figures with insets (not split axes) of relevant regions so that the reader can, as much as possible, see the raw data.

Response
Figure 5 now has split axis removed and includes an insert panel.

2. Scheme 3: Elimination of H2O doesn't give the product shown. Do you mean elimination of OH radicals? Intermediates steps are needed to show how H2O is formed.

Response
The product shown (M = 342 Da) would be formed by elimination of H_2O from AAHP, in the conversion of the peroxide unit to a carbonyl, although this is likely to be a concerted process with the combination of CI1 and ON, rather than an elementary reaction of the association complex formed from these species. We have amended the text to clarify this.

3. Define what NBS stands for at its first usage page 10 line 17.

Response
NBS is defined as Nile Blue Sulphate at first usage (page 9, line 25)

4. The ozone concentration is reported at the exit of the generator. Is this the same as the ozone concentration in the flow tube. This should be clarified.

Response
Ozone levels were measured at the exit of the aerosol flow tube, not the ozone generator (to take account of losses (negligible) and flow dilution). Chemical consumption of ozone was also found to be negligible. This is now clarified on page 7 (line 15) and page 11 (line 20).

5. The authors should discuss the possibility or not of ion-molecule reactions in the laser ionization region potentially contributing to the mass observed.

Response
The minimal residence time of the ATOFMS instrument (compared with, for example, drift-tube techniques) minimises the scope for within-detector ion-molecule chemistry to contribute to the observed signals; further confidence in this regard is achieved as the bulk of the analysis presented considers *changes* in mass spectrometric signals, upon addition of the chromophore, and particularly

as a function of the AFT chemical reaction conditions. We have added a comment to this effect in the outline of the ATOFMS applicability to this study (page 10).

6. Check Scheme 2 for consistency regarding upper and lower cases and order of name, mass etc.

Response
We have redrawn this scheme for consistency of nomenclature

7. The first part of the paper, comprising the experimental description, contains a very detailed description of the single experimental components and can be shortened for better readability.

Response
We have shortened the experimental description by ca. 1 page. But are keen to retain a sufficiently detailed description to allow repeatability (considering that this is a new experimental set-up).

9. Panel description (a, b, c) is missing in Figure 2.

Response
We have added the description (a,b,c) to the figure.

10. The comparison of NBS and NBS + OL (Figure S1b) shows next to the OL and OL dimer two additional peaks in the positive spectrum. Can you comment on their origin?

Response
As the spectrum shown is a "non-reaction" run these are likely OL fragmentation products. The masses correspond to 61 and 126.

11. Figure 3: change labeling of y-axis. Upper/lower cases in title is inconsistent with other figures, the tick label 0.0 is inconvenient, as is the position of the title. Why are the assignments for the positive ion spectrum of NN and 4-ON missing? Also the OL spectrum is different from the one in the SI, the peak around $m/z = 60$ is missing, although it does not originate from NBS.

Response
The figure has been redrawn to address the axis label clarity issues.
Mass (m/z) assignments for NN and 4-ON have been added. $m/z = 60$ had accidently been subtracted from the spectrum when subtracting the NBS signal. This has now been rectified.

12. Can you make an assumption about the nature of peaks in the positive ion spectrum in Figure 5?

Response
These peaks ($m/z = 75, 377$) do not correspond to any of the first-stage chemical reaction products discussed (or to e.g. simple linear combinations or dimers of these); without further information it is not clear that a definitive assignment can be made.

13. Define AAHP (p.21).

Response
Definition added (page 22 L6)

14. Panel description (a) is missing in Figure 7.

Response
This is added in the revised figure 7.

15. Typographical errors are noted on: p. 2 line 15, 18; p. 4, l. 23; p. 5, l. 2 (2x); p. 7,l. 17, 23; p. 8, l. 16; p. 10, l. 3; p.16, l. 1; p.21, l. 13; p. 25, l 5; p. 41

Response
All typos corrected

Referee #2

The authors have measured size dependent chemical aging of oleic acid particles under dry and humid conditions. Chemical composition was measured using an ATOFMS instrument, showing that smaller particles contain smaller products such as nonanal and oxononanoic acid, while larger particles contain more high molar mass products. Size distribution was also monitored by SMPS, demonstrating evaporation of nonanal and shrink of oxidized particles. Oleic acid – ozone system has been extensively studies both by experiments and modeling over a decade. The authors did good job in overviewing the past findings in introduction. The experiments seem to be planned carefully and conducted very well. The manuscript is written clearly and it was easy to follow. I am happy to recommend publication of this study in ACP after the below several minor comments are addressed and implemented in the revised manuscript.

Specific comments/questions:

The actual ozone concentration and reaction time are both not clearly stated. These are critical information to be specified. Ozone concentration seems to be very high (20 ppm at the O3 generator exit) with very short reaction time. This might lead to potential artifacts in ozone uptake and chemical transformation pathways of oleic acid (e.g., Renbaum and Smith, ACP, 11, 6881-6893, 2011). This issue needs to be discussed.

Response
See response to reviewer 1 and alternations to the manuscript outlined therein, which consider potential kinetic and diffusional limitations. The ozone mixing ratio in the reaction volume (where exposure to OL aerosol occurred) was 20 ppm - we have modified the manuscript (. Total reaction time is clarified (e.g. new figure 10; 20 - 135 seconds)

Was the size distribution under humid condition (presented in Fig. 2b) measured under dry conditions or same humidity as reaction conditions (65% RH) in SMPS? In other words, I am asking whether the sheath flow of SMPS was kept always dry or humidified depending on reaction conditions.

Response
The SMPS sheath flow was derived from the sampled airstream, and so reflected the same humidity. The experimental timescale (between changes in conditions) was such that ample time was available for the SMPS to relax to changes in RH.

It seems that exposure (time * O3 concentration) was not large enough to react away all of oleic acid molecules (13-31% of OL remained unreacted in Fig. 7&8). Have you tried to increase exposure? Would particles evaporate even more in that case? Is it possible for authors to present the evolution of particle size (or mass) as a function of reaction time or particle size dependence on O3 concentration?

<u>Response</u>
See response to reviewer 1, above, and new manuscript figures 9 and 10, which show essentially complete (within measurement uncertainty) and first-order consumption of OL

P18, L20: Do authors have any evidence to believe it is the primary ozonide, but not secondary ozonide? Is POZ stable enough to be detected by ATOFMS?

<u>Response</u>
There is no experimental evidence, hence our caution in stating this peak *could* be assignable to the POZ. To our knowledge, there are no thermochemical data re the stability of ozonides of this size available, let alone in the OL/NBS particle matrix, so we are reluctant to speculate.

P23, L10: There seems to be misunderstanding of explanation of Shiraiwa et al. (2010). They did not show large concentration gradient of OL in the bulk, but actually they showed OL is homogeneous in the bulk due to rapid bulk diffusion. Ozone can be constrained in the near-surface bulk due to reactions with oleic acid.

<u>Response</u>
We have revised the phrasing (P24 L6) of the manuscript in this section. We are in agreement with the reviewer.

P15, L17: Can you quantify OL dimer? Did it disappear after exposure to ozone? Could it potentially affect reaction kinetics/pathways (e.g., Fig. 9, Zahardis & Petrucci, 2007)?

<u>Response</u>
We cannot quantify the dimer as no standards are available, and the response may differ from (e.g.) OL or the other quantified products - hence we focus upon the kinetics of OL alone. We cannot preclude reactions of the dimer affecting the products formed, and have added a caveat to this effect (page 20 L25).

References

Hearn, John D., and Geoffrey D. Smith. "Kinetics and product studies for ozonolysis reactions of organic particles using aerosol CIMS." *The Journal of Physical Chemistry A* 108.45 (2004): 10019-10029.

Moise, Tamar, and Yinon Rudich. "Reactive uptake of ozone by proxies for organic aerosols: Surface versus bulk processes." *Journal of Geophysical Research: Atmospheres* 105.D11 (2000): 14667-14676.

Hearn, John D., Amanda J. Lovett, and Geoffrey D. Smith. "Ozonolysis of oleic acid particles: evidence for a surface reaction and secondary reactions involving Criegee intermediates." *Physical Chemistry Chemical Physics* 7.3 (2005): 501-511.

Thornberry, T., and J. P. D. Abbatt. "Heterogeneous reaction of ozone with liquid unsaturated fatty acids: detailed kinetics and gas-phase product studies." *Physical Chemistry Chemical Physics* 6.1 (2004): 84-93.

Ziemann, Paul J. "Aerosol products, mechanisms, and kinetics of heterogeneous reactions of ozone with oleic acid in pure and mixed particles." *Faraday Discussions* 130 (2005): 469-490.

Knopf, Daniel A., Lori M. Anthony, and Allan K. Bertram. "Reactive uptake of O3 by multicomponent and multiphase mixtures containing oleic acid." *The Journal of Physical Chemistry A* 109.25 (2005): 5579-5589.

SIZE DEPENDENT CHEMICAL AGEING OF

OLEIC ACID AEROSOL UNDER DRY AND HUMIDIFIED

CONDITIONS

Suad S. Al-Kindi, Francis D. Pope*, David C. Beddows[‡],

William J. Bloss and Roy M. Harrison[†‡]

School of Geography, Earth and Environmental Sciences

University of Birmingham

Edgbaston, Birmingham B15 2TT

---

* Corresponding author: f.pope@bham.ac.uk
[†] Also at: Department of Environmental Sciences / Center of Excellence in Environmental Studies, King Abdulaziz University, Jeddah, 21589, Saudi Arabia
[‡] Also at: National Centre for Atmospheric Science, United Kingdom

United Kingdom

ABSTRACT

A chemical reaction chamber system has been developed for the processing of oleic acid aerosol particles with ozone under two relative humidity conditions: dry and humidified to 65% R.H. The apparatus consists of an aerosol flow tube, in which the ozonolysis occurs, coupled to a scanning mobility particle sizer (SMPS) and an aerosol time-of-flight mass spectrometer (ATOFMS) which measure the evolving particle size and composition. Under both relative humidity conditions, ozonolysis results in a significant decrease in particle size and mass which is consistent with the formation of volatile products that partition from the particle to the gas phase. Mass spectra derived from the ATOFMS reveal the presence of the typically observed reaction products: azaleic acid, nonanal, oxononanoic acid and nonanoic acid, as well as a range of higher molecular weight products deriving from the reactions of reaction intermediates with oleic acid and its oxidation products. These include octanoic acid, and 9- and 10-oxooctadecanoic acid, as well as products of considerably higher molecular weight. Quantitative evaluation of product yields with the ATOFMS shows a marked dependence upon both particle size association (from 0.3 to 2.1 µm diameter) and relative humidity. Under both relative humidity conditions, the percentage residual of oleic acid increases with increasing particle size and the main lower molecular weight products are nonanal and oxononanoic acid. Under dry conditions, the percentage of higher molecular weight products increases with increasing particle size, due to the poorer internal mixing of the larger particles. Under humidified conditions, the percentage of unreacted oleic acid is greater, except in the smallest particle fraction, with little formation of high molecular weight products relative to the dry particles. It is postulated that water reacts with reactive intermediates, competing with the processes which produce high molecular weight products. Whilst the oleic acid model aerosol system is of limited relevance to complex internally mixed atmospheric aerosol, the generic findings presented in this paper give useful insights into the nature of heterogeneous chemical processes.

1. INTRODUCTION

Atmospheric aerosol particles play critical roles in air quality, visibility, human health, regional and global climate, cloud condensation nuclei ability, precipitation events, atmospheric acid deposition, optical properties, atmospheric energy balance, and stratospheric ozone depletion (Harrison, 2014). Aerosol particles are typically composed of a mixture of inorganic and organic material. The organic component of aerosol is highly complex and may contain thousands of different chemical species of both biogenic and anthropogenic origin (Goldstein and Galbally, 2007). These organic components cause aerosol particles to exhibit a wide range of chemical properties due to their differing composition.

Primary organic aerosol (POA) particles are emitted directly from anthropogenic and biological sources (Pöschl, 2011). It is composed of a wide range of hydrocarbons, partially oxidized organics, and elemental carbon primarily related to combustion processes including burning of fossil fuels, cooking, domestic heating, and biomass burning. Natural biogenic sources of organic aerosol particles include plants and vegetation, the ocean surface, volcanic eruptions, and wind-driven dust (Pöschl, 2011). By contrast, secondary organic aerosol (SOA) particles are formed in the atmosphere from biogenic and anthropogenic gaseous precursors. Several pathways for the transformation of aerosol particles in the atmosphere have been identified, which may alter their chemical and physical properties, in general causing hydrophobic-to-hydrophilic conversion of organic components. These pathways include gas-phase reactions, condensed-phase reactions, multiphase reactions, and multigenerational chemistry which has received attention recently because it is the least understood (Rudich, 2003; Petters et al., 2006; Kroll and Seinfeld, 2008; Carlton et al., 2010; Koop et al., 2011; Kolb and Worsnop, 2012).

The ozonolysis of oleic acid (OL) aerosol is a much studied heterogeneous reaction which provides a readily accessible test system for the understanding of atmospheric processing of organic aerosol under a range of environmental conditions (Hearn and Smith, 2004; Katrib et al., 2004; Ziemann, 2005; Gonzalez-Labrada et al., 2007; Zahardis and Petrucci, 2007; Vesna et al., 2009; Pfrang et al., 2010; Lee et al., 2012; Chan et al., 2013; Hosny et al., 2013; Mendez et al., 2014; Hosny et al., 2016) - although oleic acid itself is only introduced into the atmosphere in small quantities via the heating of fat and cooking oil. OL studies have, for example, explored the effects of the droplet state (Katrib et al., 2005a), relative humidity (RH) (Vesna et al., 2009; Lee et al., 2012), OL and ozone concentration (Lee and Chan, 2007; Mendez et al., 2014), and extent of chemical ageing (Reynolds et al., 2006) upon the OL - ozone system. The kinetics (Moise and Rudich, 2002; Gonzalez-Labrada et al., 2007), reaction mechanism and products (Hearn and Smith, 2004; Katrib et al., 2004; Hung et al., 2005; Zahardis et al., 2005; Ziemann, 2005; Zahardis et al., 2006; Zahardis and Petrucci, 2007, Wang et al., 2016), particle morphology and hygroscopicity (Dennis-Smither et al., 2012a), and viscosity (Hosny et al., 2013; 2016) have also been investigated.

The initial stages in the mechanism of particulate phase OL ozonolysis are comparatively well understood (Moise and Rudich, 2002; Smith et al., 2002; Hearn and Smith, 2004; Katrib et al., 2004; Ziemann, 2005; Grimm et al., 2006; Nash et al., 2006; Hung and Ariya, 2007; Zahardis and Petrucci, 2007; Vesna et al., 2008; Lee et al., 2012), see Scheme 1. The initial step in the reaction is the addition of ozone across the double bond of OL forming an unstable primary ozonide (POZ). Subsequently, the POZ decomposes, via two potential routes, through cleavage of the C-C bond alongside one of the two O-O bonds. Both routes generate an aldehyde and an excited Criegee Intermediate (CI) as products, but with differing chemical identity depending upon which O-O bond is broken. In reaction route 1 (Scheme 1), nonanal (NN) and CI1 are formed; the CI1 can isomerise to form stabilized azelaic acid (AA), a cyclic

acyloxy hydroperoxide (CAHP), or octanoic acid (OcA) and carbon dioxide (Gonzalez-Labrada, Schmidt et al. 2007). Alternatively, CI1 may be scavenged via numerous potential association reactions with the co-produced aldehyde, other carboxylic-functionalised moieties, (further) OL molecule double bonds, solvents or via self-reaction. This extensive secondary chemistry reflects the reactivity of CIs (Zahardis and Petrucci, 2007). Similarly, in reaction route 2, oxo-nonanoic acid (ON) and excited Criegee Intermediate 2 (CI2) are formed, and CI2 decomposes by forming stabilized nonanoic acid (NA), or may be scavenged via similar pathways as described above for CI1. The principal reaction products of OL ozonolysis are therefore NN, AA, ON, and NA. There are also numerous reports in the literature of the formation of higher molecular weight products (Hung et al., 2005; Reynolds, et al., 2006; Zahardis et al., 2005) including esters (Hung et al., 2010) and peroxides (Reynolds et al., 2006; Vesna et al., 2009; Zahardis et al., 2005; 2006; Ziemann, 2005). Although OL is essentially hydrophobic, the reaction products are hydrophilic (Lee et al., 2012).
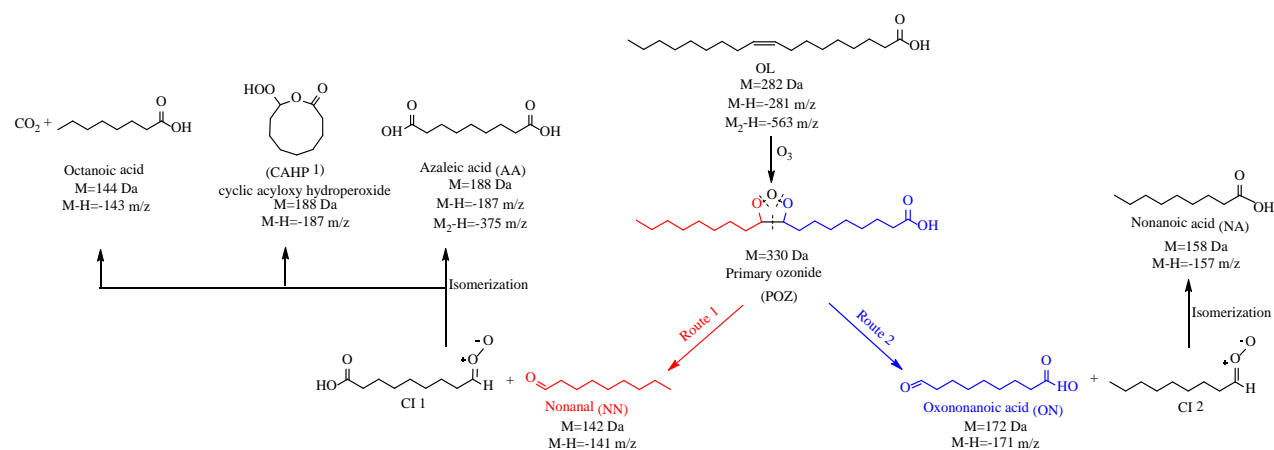
Scheme 1: Initial steps and primary products of Oleic Acid (OL) oxidation by O_3.

This study investigates the chemical mechanisms of OL ozonolysis and the resulting product distribution, assessed as a function of particle size using a variety of novel online physical and chemical analysis methodologies. The effect of relative humidity upon the (size dependent)

predominant reaction mechanism is also explored, and the resulting implications for the atmospheric processing of organic aerosol are considered.

2. EXPERIMENTAL

2.1 Experimental Design

A schematic diagram of the experimental setup for the ozonolysis of OL aerosol is shown in Figure 1. The system comprised a gas handling and control system, an aerosol generator, ozone generator, humidifier (bubbler), and an aerosol flow tube (AFT), coupled to aerosol particle characterisation (SMPS - Scanning Mobility Particle Spectrometer - and ATOFMS - Aerosol Time-of-Flight Mass Spectrometer) instruments, and monitors to measure ozone, temperature and relative humidity (RH). The setup was designed so the ozonolysis of OL aerosol could be studied under well-defined conditions within the AFT.

The AFT reactor consisted of a cylindrical tube formed from Pyrex (internal diameter = 10 cm, length = 100 cm) which was sealed with aluminium flanges. The reactor was held in a vertical orientation within a supporting frame. Gas inlets and outlets were coupled to the flanges to allow for the entrance and exit of the gas and aerosol streams. The ozone monitor, SMPS and ATOFMS sampling outlets were located immediately downstream of the AFT. Typical gas flows entering the AFT were as follows : OL aerosol containing flow (1.0 slm in synthetic air), ozone containing dry synthetic air (0.5 slm), and dry or humidified synthetic

air (2.0 slm) resulting in a total flow rate of 3.5 slm which corresponded to a (plug flow) residence time of 135 s. In some experiments a nitrogen flow was used to generate the aerosol (via homogeneous nucleation of OL); in these cases a small flow of oxygen was added to ensure the air composition within the AFT had an atmospheric $N_2:O_2$ ratio. Constant gas flows were achieved using calibrated mass flow controllers. The Reynolds number for the AFT was 13.1 and hence flow within the reactor was predicted to lie firmly within the laminar regime after an initial flow development length (estimated at 4.6 cm, i.e. < 5% of the total length).

.

To ensure that particle processing was dominated by the AFT section of the setup, the additional residence time within the sampling and characterisation stages was assessed. The calculated residence time of the aerosol in the sampling tubes (<2 s) and SMPS (<1 s) (von Hessberg et al., 2009) was negligible. Within the ATOFMS the residence time is very small, and the low operating pressures within the ATOFMS ($\sim 10^{-7}$ Torr) minimize interactions between ozone and particles, and hence particle reactivity is considered to be terminated at the very early stages of the ATOFMS sampling nozzle.

A hygrometer probe positioned inside the AFT was used to monitor RH and temperature. Experiments were typically run under both dry and humidified conditions which corresponded to measured relative humidities of 0.5±0.02 % and 65.0±0.2%, respectively.

Each experiment was run back-to-back with and without the presence of ozone, with all other conditions remaining identical, to allow measurement of both the initial OL particles before

ozonolysis and the resulting aerosol post ozonolysis. Measurements were conducted once the aerosol concentration, size distribution and ozone concentration had stabilised. The system was flushed between runs to prevent contamination from prior experiments.

2.2   Scanning Mobility Particle Sizer (SMPS)

To follow changes in the OL particle size distribution due to ozonolysis, an SMPS system comprising an electrostatic classifier (TSI model 3080), neutralizer (TSI model 3076), long column differential mobility analyzer (LDMA, TSI Model 3081) and condensation particle counter (CPC, 3022A) was used to monitor the aerosol size distribution. A particle density equal to that of pure OL (0.891 g cm^{-3}) was applied to determine changes in the number, diameter, volume and mass distribution of OL particles. Aerosols were monitored in the size range of 15.1 – 667 nm, every 3 minutes, before and after exposure to ozone. For each experimental setting, a minimum of 10 sizing scans were averaged.

2.3   Aerosol Time of Flight Mass Spectrometer (ATOFMS)

A detailed description of the ATOFMS is given elsewhere (Gard et al., 1997; Sullivan and Prather, 2005; Dall'Osto et al., 2006); briefly, the ATOFMS is an on-line single particle instrument which was applied here to measure the physical and chemical characteristics of OL aerosol before and after ozonolysis. The ATOFMS deployed in this study (TSI, Model 3800-100) sampled particles in the size range 100 – 3000 nm. For analysis of individual particle composition, time of flight mass spectrometry (TOF-MS) was used with a laser (266 nm) desorption ionization (LDI) source.

The ATOMFS sampled from the AFT at a flow rate of 0.3 slm. When an aerosol flow enters the ATOFMS it is directed through an expansion nozzle and skimmers during which particles are

accelerated to a velocity characteristic of their aerodynamic size; the smaller the particle the higher

the speed. Velocities of individual particles, hence aerodynamic size, are measured via scattered

light from two CW timing lasers (532 nm) positioned a known distance apart. The particle velocity

determines the timing of the subsequent LDI pulse to allow for interaction between particles and

LDI. Once ionized, the molecular fragments from the particle are directed to both positive and

negative polarity time-of-flight mass spectrometers.

The detection of particles within the ATOFMS is reliant upon the LDI pulse generating ions,

requiring the particle to have sufficient absorption properties at 266 nm. We found that the

interaction between the LDI and both OL and its ozonolysis products produced only

negligible ions, failing to meet the detection criteria of ATOFMS. To increase the absorption

properties of the particles, the dye Nile Blue Sulphate (NBS) was introduced into the OL

particles. NBS effectively absorbs light at the lasing wavelength of the LDI laser with

absorption peaks occurring at 624, 325 and 276 nm) and therefore its introduction into the

aerosol provides a methodology for efficient ionization. NBS was also separately introduced

into calibration particles formed from each of the primary products of OL ozonolysis (See

Results section).

Although the ATOFMS response is matrix-sensitive and may not directly reflect the

quantitative composition of the measured aerosol (Gross et al., 2000; Fergenson et al., 2001;

Bhave et al., 2002; Sullivan and Prather, 2005; Allen et al., 2006; Dall'Osto et al., 2006),

relative peak intensities can be meaningful when particle constitution within a measured

sample has not changed considerably during a given investigation (Gard et al., 1998;

Finlayson-Pitts and Pitts, 2000). In this sense, the use of ATOFMS as a semi-quantifiable

approach for the analysis of aged OL particles as a function of particle size is justifiable

because individual laboratory based particles studied under experimentally controlled conditions are far less complex - and variable - than atmospheric aerosol (Allen, 2004). Moreover, ATOFMS information on particle number and the abundance of different species by particle size are possible with high time resolution (Dall'Osto and Harrison, 2012). Most importantly, the relative signal intensities arising from the major oxidation products of the OL-O_3 heterogeneous reaction were studied using individual authenticated standards, the analysis of which was used to calibrate signals arising from reacted oleic acid particles. The minimal residence time of the ATOFMS instrument (compared with, for example, drift-tube techniques) minimises the scope for within-detector ion-molecule chemistry to contribute to the observed signals; further confidence in this regard is achieved through the focus upon changes in signal upon addition of the chromophore, and as a function of chemical reaction conditions (in comparison with a focus upon direct spectra).

The ATOFMS particle sizing was calibrated with standardized polystyrene latex spheres (PSL, calibrated diameters = 0.2, 0.3, 0.4, 0.56, 0.7, 1.3, 2, and 2.5 μm). Dilute PSL suspensions were prepared in deionised water and nebulised using a constant output atomiser and diffusion dryer. Analysis of the measured velocity of the nebulised PSL particles as a function of their known particle sizes provided a calibration curve for the ATOFMS particle sizing.

The mass scale of the ATOFMS was calibrated through nebulisation of two multi-element commercial standards (see Chemicals and Reagents, below) and further standards prepared for this study reflecting the principal products of the OL ozonolysis system : OL, AA, NN, NA and 4-oxononanoic acid (4-ON) together with NBS (added chromophore). The obtained time of flight of the resulting ions in each case was related to the corresponding expected m/z

values. This approach allowed for the ATOFMS response to be directly calibrated up to 563 Da. m/z values reported here beyond this limit have been calibrated using the molecular masses for those higher molecular weight products for which identities have been proposed. To assess the relative sensitivity of the ATOFMS towards OL, NN, AA, NA and 4-ON, a standard mixture solution containing OL, NN, AA, NA, and 4-ON at equimolar concentrations, plus traces of the laser dye, NBS, was prepared in methanol and aerosolized using liquid atomisation. The ATOFMS datasets were all processed using MS Analyse and Microsoft Access software.

2.4   Generation and Measurement of OL Aerosol and Ozone

Ozone was generated by flowing 0.5 slm of synthetic air through a quartz photolysis tube illuminated by a mercury UV pen-ray lamp The ozone concentration was monitored downstream of the AFT using an ozone monitor (2B Technologies, Model 205). The ozone mixing ratio was 20 ppm. An elevated O_3 level allows use of short contact times in the AFT and corresponds to an integrated exposure approximately equivalent to about one day in ambient air [if potential within-particle diffusion limitations may be neglected].

Two approaches were used to generate OL aerosol. For the physical characterisation of OL aerosol using the SMPS, liquid OL particles were generated by homogenous nucleation of pure OL vapour. The low-volatile OL liquid was heated in a Pyrex vessel, in an insulated and temperature-controlled oven (120±0.5 °C), to create OL vapour. To aid evaporation 0.5 slm of N_2 gas was bubbled through the liquid OL. Subsequently, the vapour underwent homogeneous nucleation into OL aerosol particles accelerated by the introduction of a 0.5 slm flow of N_2 gas at ambient temperature. The resulting aerosol stream was passed through a reheating tube (200 °C) to homogenise the aerosol and narrow the resulting particle size distribution. All steps in the procedure were kept at

temperatures significantly below the boiling point of OL (360 °C) to prevent pyrolysis. Overall, these operating conditions generated OL aerosols with a geometric standard deviation σ_g of 1.2, a mass median diameter close to 400 nm and a total particle number concentration of ~10^6 cm^{-3}.

For the chemical product study of OL aerosol using the ATOFMS, a different method for generating OL aerosol was required as a consequence of the necessity of doping the aerosol with NBS dye (see discussion above). NBS was added at a low concentration (5×10^{-5} M) to liquid OL and the mixture made up into 0.15 M solutions of OL in methanol. Subsequently, a constant output atomiser (TSI, Model 3076) was used to generate a polydisperse aerosol ensemble from the solution. The atomiser requires a constant flow rate of 3.0 slm for operation. Of this aerosol-containing flow, 1.0 slm was directed into the AFT after it passed through a series of two silica gel diffusion dryers (TSI: Model 3062) for the removal of methanol prior to entry to the AFT, while the remaining flow was vented. Under the experimental conditions of this study, methanol is expected to fully evaporate and indeed no methanol signal was detected in any of the ATOFMS mass spectra. Generation of the other aerosols containing NBS (i.e. calibration standards) was performed in the same manner.

2.5   Chemicals and Reagents

Liquid OL (purity > 99.0%), solid crystalline azelaic acid (AA, 98%), liquid nonanal (NN, 95%), liquid nonanoic acid (NA, 96%) and liquid 4-oxononanoic acid (4ON, 95%) were purchased from Sigma-Aldrich and used as supplied. For ATOFMS mass calibration, multi-element standard solutions were used: standard A (900 μg/ml: Ba, Pb, Li, K, Na & V in 5% HNO$_3$) and standard B (900 μg/ml: Ag and Mo in 5% HNO$_3$) obtained from TSI Inc. The size calibration of the ATOFMS used polystyrene latex spheres (PSL, diameter range: 0.1 to

2.5 µm, Duke Scientific). The cationic laser dye, bis[5-amino-9-(diethylamino)benzo[a]phenoxazin-7-ium] sulphate, Nile Blue Sulphate (NBS), used to modify the spectroscopic properties of OL particles and laboratory grade methanol were obtained from Fisher Scientific. Synthetic air and nitrogen free oxygen (N_2) (99.9% stated purity) were supplied by BOC and purified by passing through charcoal traps (Grace Discovery Science, Efficiency<20 ppb) to remove trace hydrocarbon impurities. Traces of water were removed from the gas lines using a trap (Sigma-Aldrich, Molecular Sieve 5A Moisture Trap).

3.   RESULTS

3.1   Effect of Ozonolysis on Particle Size

The size distributions of ozonolysed and non-ozonolysed OL particles, under both dry and humidified conditions, are shown in panels (a) and (b) in Figure 2. To aid comparison, the wet and dry results are combined, and normalized to the peak signal of the non-processed particle, in Figure 2 panel (c). It can be clearly observed that OL particles lose mass upon oxidation under both dry and humidified conditions. The modal diameter decreases from 400±14 to 346±13 nm and from 372±13 to 322 ±12 nm under the dry and humidified conditions, respectively, corresponding to a total mass loss (estimated from the SMPS) of 32.5±5.3% and 26.3±2.5% respectively. Although the observed mass loss upon oxidation is consistent with previously reported qualitative and quantitative observations (Morris et al., 2002; Katrib et al., 2004; Katrib et al., 2005b; Dennis-Smither et al., 2012b; Lee et al., 2012), in view of the measured uncertainties the difference between the two experiments, under

different RH conditions, is statistically insignificant. The lack of hygroscopic growth of the initial OL

aerosol is consistent with the observations of Dennis-Smither et al. (2012a) and Hung et al. (2005).

The decrease in the mobility diameter of OL particles upon oxidation is likely due to the

formation of volatile products that partition from the particle to the gas phase. This is

consistent with previous studies that have identified gas phase products. In particular the

highly volatile nonanal (NN) and the semi-volatile nonanoic acid (NA) products have been

previously identified (Moise and Rudich, 2002; Smith et al., 2002; Thornberry and Abbatt,

2004; Vesna et al., 2009; Lee et al., 2012). The formation of low volatility products, which

remain in the particle phase, and typically possess greater densities (ρ) than OL (ρ = 0.891 g

cm^{-3}), such as azelaic acid (AA, ρ =1.225 g cm^{-3}) and 9-oxononanoic acid (ON, ρ = 1.019 g

cm^{-3}) may also have an influence.

The fact that less mass loss was observed under humidified conditions than under dry

conditions (although the difference was statistically insignificant), suggests that the presence

of water might have an effect on the oxidation mechanism. Such a conclusion has been

reported in the literature for similar oxidation conditions (Gallimore et al., 2011). It has been

suggested that the presence of particle phase water leads to different CI reactivity (i.e. an

alternate CI fate) which results in the formation of less volatile products (such as organic acid

formation) and hence less particle mass loss (Gallimore et al., 2011). This is surprising

because OL and its oxidation products, even though they are smaller and contain more

hydrophilic chemical moieties (carboxylic acid and hydroxyl groups), have low solubility in

water. Results from other experimental studies indicate that OL has mild hygroscopicity

(Andrews and Larson, 1993; Kumar et al., 2003; Vesna et al., 2008) Furthermore

thermodynamic modelling indicates that OL and ozonolysed OL particles show small but

non-negligible hygroscopicity at RH 65% (Lee et al., 2012). It should be noted that hygroscopicity is defined by mass or diameter growth upon uptake of water referenced to the dry state. Since the molar mass and molar volume of water is much smaller than OL and its oxidation products, the molar ratio of water to OL or its oxidation products is much greater than the reported hygroscopicity would suggest. Dennis-Smither et al. (2012a,b) report a reduction in particle size with oxidation of OL and that hygroscopicity increases with oxidative aging. While Lee et al. (2012) observed no change to the reaction scheme of OL with increased humidity, Vesna et al. (2009) report changes in product yields.

3.2 Chemical Characterisation of OL and Ozonolysed OL Aerosol

Particles leaving the AFT were sampled by the ATOFMS. Ionisation within the instrument leads to ions which enter two time-of-flight mass spectrometers. Both positive and negative mass spectra were recorded for all detected particles. The negative mass spectra show a greater abundance of peaks which is expected based upon the predicted reaction pathways (see Scheme 1) because most OL oxidation products contain carboxylic acid and/or aldehyde moieties which are principally detected as deprotonated molecular ions [M-H]$^-$ formed via proton abstraction. To allow easier interpretation and minimise fragmentation, the LDI laser fluence of the ATOFMS was kept very low (0.4–0.8 mJ per pulse) as compared to other studies (1.3–1.6 mJ) (Silva and Prather, 2000; Dall'Osto and Harrison, 2012). Nevertheless, it should be noted that some fragmentation of ions in the ATOFMS system is expected and this can lead to difficulty in interpretation.

3.3 Mass Spectrometric Analysis of NBS and OL

To probe for any influence of NBS on the chemistry of OL ozonolysis two preliminary tests were carried out. Firstly the mass spectra of NBS aerosol with and without O$_3$ present were

recorded (Figure S1a). Secondly the mass spectrum of aerosol composed of NBS and OL

without O_3 was recorded (Figure S1b). NBS displays three strong signals in the positive

spectrum at m/z +274 and +308 assigned to the cationic dye fragments and +318 assigned for

the non-fragmented dye cation. The two strong signals in the negative spectra at m/z -96 and

-80 correspond, respectively, to the sulphate (SO_4^{2-}) and sulphite (SO_3^{2-}) ions of the dye. No

changes in the NBS spectra were detected when NBS particles were exposed to ozone (Figure

S1a). When OL was added to NBS solution in the absence of ozone, the only additional

peaks observed were the deprotonated mass signals from OL and the OL dimer. It should be

noted that NBS peaks were always observed in all mass spectra shown henceforth. However,

for the ease of the analysis, all NBS peaks are omitted from the presented mass spectra.

3.4   Mass Spectrometric Analysis of OL Oxidation Products

In order to quantify the products of OL ozonolysis the relationship between the mass spectral

signal and the concentration needs to be quantified. Standards for OL, AA, NN and NA were

all commercially available. However, ON was not commercially available but its isomer 4-

oxononanoic acid (4-ON) was. The detection of ON via the ATOFMS is expected to be near-

identical to that of 4-ON. ON contains a carboxylic acid and an aldehyde group whereas 4-

ON contains carboxylic acid and ketone groups. Both acids, derived from ON and 4-ON, are

expected to exhibit a deprotonated carboxylate ion [M-H]$^-$ and were detected in the negative

ion mass spectrum at m/z -171. Standards for the high molecular weight oxidation products

are not available commercially and are difficult to synthesise and hence were unavailable for

this study.

Figure 3 shows the positive and negative mass spectra of the individual standards. Unreacted

OL aerosol (282 Da) was seen as a deprotonated OL molecular ion at m/z = -281 and as a

singly deprotonated dimer at m/z -563. The deprotonated molecular ions of AA (MW = 188 Da), NA (158 Da), NN (142 Da) and 4-ON (172 Da) are seen as major peaks at m/z -187, -157, -141 and -171 respectively, while the singly deprotonated dimers of AA and NA were measured at m/z -375 and -315, respectively. In the positive ion mass spectra of AA a signal at m/z +155 was attributed to the fraction of the molecule after the loss of an HO_2 fragment $[M-HO_2]^+$. The molecular ion peak measured at m/z +113 in the NA positive ion mass spectra was assigned to the molecular fragment of NA after the loss of CO_2H, $[M-CO_2H]^+$. It is important to note that the ATOFMS intensity for individual ions is dependent upon the total composition of the particle.

To investigate ATOFMS sensitivity towards OL and the primary ozonolysis products, a solution containing an equimolar mixture of OL, AA, NA, NN and 4-ON was examined under the same experimental conditions as the oxidation experiments. Figure 4 shows the results of the ATOFMS (relative) sensitivity to the deprotonated molecular ions of the five component mixture. An average spectrum comprised of 200 spectra was used for the analysis. It is evident that the ATOFMS sensitivity varies considerably between the different compounds.

The figure indicates that the signals observed for the five component mixture is in the following order: AA >> ON > OL > NA > NN. The much greater signal from AA compared to the other species can be partially understood because it is a dicarboxylic acid and thus has a greater possibility of being ionized to the carboxylate ion compared to the species containing only one carboxylic acid moiety. ON and OL have similar signals which is expected since they both contain one carboxylic acid group. The signal from NN is the smallest probably because it only contains an aldehyde moiety which is more difficult to

ionize compared to carboxylic acids. Previous studies on NN detection using soft ionisation and ultra-high resolution mass spectrometry also showed weak NN peaks in the mass spectra. The authors attribute this observation partly to the poor signal produced from aldehydes by the deployed techniques (Grimm et al., 2006; Hosny et al., 2013). The high volatility of NN will also lead to the partitioning from the aerosol to gas phase thereby reducing the particle phase concentration, although it is noted that this process will also happen in the processed oleic acid particles.

The relative peak areas of the five component mixture were converted into sensitivity correction factors (SCF) that allow for relative concentrations of these components to be estimated within the ozonolysed OL particles. It should be noted that this approach – as in many other analytical approaches – is not sensitive to any matrix effect of ozonolysed OL particles which might have an impact of suppressing or enhancing ATOFMS signals of individual components. To minimize possible matrix complications, the relative peak intensities of the individual components within each measured sample were used to describe the component distribution of the chemically aged OL polydisperse aerosol. As mentioned in Section 2.3, satisfactory ATOFMS measurement of the aged OL particles required improving the efficiency of the LDI by optically modifying the matrix of OL particles using added NBS laser dye. This modification resulted in a substantial enhancement in ATOFMS detection of particles apparently by maximising the absorption efficiency of the pulsed laser by the particles.

3.5   Mass Spectrometric Analysis of Aged OL Particles

The size binned ATOFMS data show distinct differences in composition between small particles ($D_p<0.3$ µm) and large particles ($D_p>0.3$ µm). Small particles are characterised by the presence of compounds with molecular weights lower than the parent OL molecules (m/z<282), whereas large particles are characterised by significant formation of higher molecular weight (HMW) compounds (m/z>282). Smith et al. (2002) measured ozone uptake by OL particles as a function of particle size. They found that the effective uptake coefficient of ozone decreased with increasing particle size, concluding that this resulted from the reaction being limited by the diffusion of OL within the particle. Under such conditions, reactions between intermediate products and OL become important, hence leading to the formation of higher molecular weight species (Hung et al., 2005; 2007; Katrib et al., 2004). Reactions between ozonolysis products and Criegee intermediates also lead to high molecular weight products when the supply of ozone is limited (Reynolds et al., 2006; Zahardis et al., 2006). Our interpretation of the mass spectral information gained from the ATOFMS appears in Table 1.

3.6 Mechanisms and Mass Spectrometric Analysis of Small Particles

The mass spectrum of small oxidised OL particles (average of 300 spectra) is shown in Figure 5. In addition to the parent OL signal measured at m/z -281, three of the primary ozonolysis products: AA, ON, and NA, were observed at m/z -187, -171 and -157, respectively. Peaks measured at m/z=-143, -329 and -439 could be indicative of octanoic acid (OcA) (144 Da), the primary ozonide (POZ), (see Scheme 1) and the secondary reaction product of CI2 with OL (reaction R 1), respectively. The unidentified mass spectrum peaks are likely due to fragments (daughter ion peaks) or aggregates of ions. No useful insights were gained from the positive mass spectrum.

Addtion to OL carboxylic moiety

CI 2

M=440 Da
M-H=-439 m/z
M-HO$_2$=+423 m/z
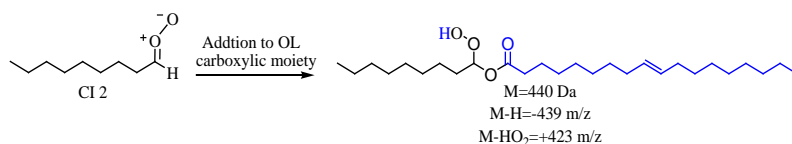
R 1

3.7 Mechanisms and Mass Spectrometric Analysis of Large Size Particles

The three frames, a, b, and c, in Figure 6 show negative and positive ion mass spectra of large ($D_p > 0.3$ µm) aged OL particles (average of 700 spectra). The negative ion mass spectrum is more complex but compatible with the hypothesis of secondary chemistry and the formation of HMW products. Generally, the spectrum demonstrates a strong peak of unreacted parent OL at m/z -281 and the appearance of the major oxidation products of ozone exposure. All four primary products (AA, ON, NA and NN) are found to be in the particle phase including the highly volatile NN which was not detected in the small particles. The presence of NN in large particles is consistent with the observations of Dennis-Smithers et al. who studied supermicron sized particles (Dennis-Smither et al., 2012b). The signals of AA and OcA which form through the molecular rearrangement of CI1, were not detected in the larger particles, which might reveal that isomerization is predominant in smaller particles and that it is the only formation source for these products. Both negative and positive average mass spectra are characterized by the presence of HMW products presumably formed by secondary association reactions of primary reaction products.

Previous studies have reported evidence of secondary chemistry occurring within the ozonolysis of OL particles (Katrib et al., 2004; Hearn et al., 2005; Ziemann, 2005; Reynolds et al., 2006; Zahardis et al., 2006; Zahardis and Petrucci, 2007; Lee et al., 2012; Hosny et al., 2013). The presence of the liquid condensed phase substrate for the CIs minimizes their molecular rearrangement (Katrib et al., 2004) via a solvent cage effect (Park et al., 2006) and maximizes their lifetimes. Therefore, reaction probability of CIs with their corresponding

carbonyl compounds to form secondary ozonide (SOZ) or with the alkene functionality becomes more significant (Neeb et al., 1998; Moise and Rudich, 2002; Zahardis et al., 2005). Table 1 proposes molecular structures for the observed HMW mass spectral signals based upon polymerization mechanisms previously proposed in the literature (Smith et al., 2002; Hearn and Smith, 2004; Katrib et al., 2004; Hung et al., 2005; Zahardis et al., 2005; Reynolds et al., 2006; Zahardis et al., 2006; Hung and Ariya, 2007; Zahardis and Petrucci, 2007). For instance, the peak at m/z -297 can be assigned for two isomeric compounds, 9-oxooctadecanoic acid (Ox1) or 10-oxooctadecanoic acid (Ox2), depending on the type of the CI formed and the geometry of the CI addition across the double bond of OL to form the C_{27} peroxide which can cleave to yield the primary products ON or NN. Similarly, the detected signal at m/z -327 is determined as a reaction product between the OL double bond and CI1 to form 9-oxooctadecanedioic acid (Ox3). Scheme 2 illustrates a proposed mechanism and product structures formed as a result of the reaction between CI1 and the alkene functionality of OL. The experimental and modelling studies by Wang et al. have shown that the addition of CIs across the double bond of OL is the dominant loss route of CIs in OL-O_3 heterogeneous reaction system (Wang et al., 2016). We note that other reactions may also contribute to the observed products - for example, fates of the OL dimer - which these experiments cannot definitively constrain.

The presence of peaks correspond to Ox1 or Ox2 in the OL-O_3 heterogeneous reaction has been reported previously (Hearn and Smith, 2004; Zahardis et al., 2006; Hung and Ariya, 2007) while the reaction mechanism and product structures were first hypothesized by Katrib and co-workers (Katrib et al., 2004).
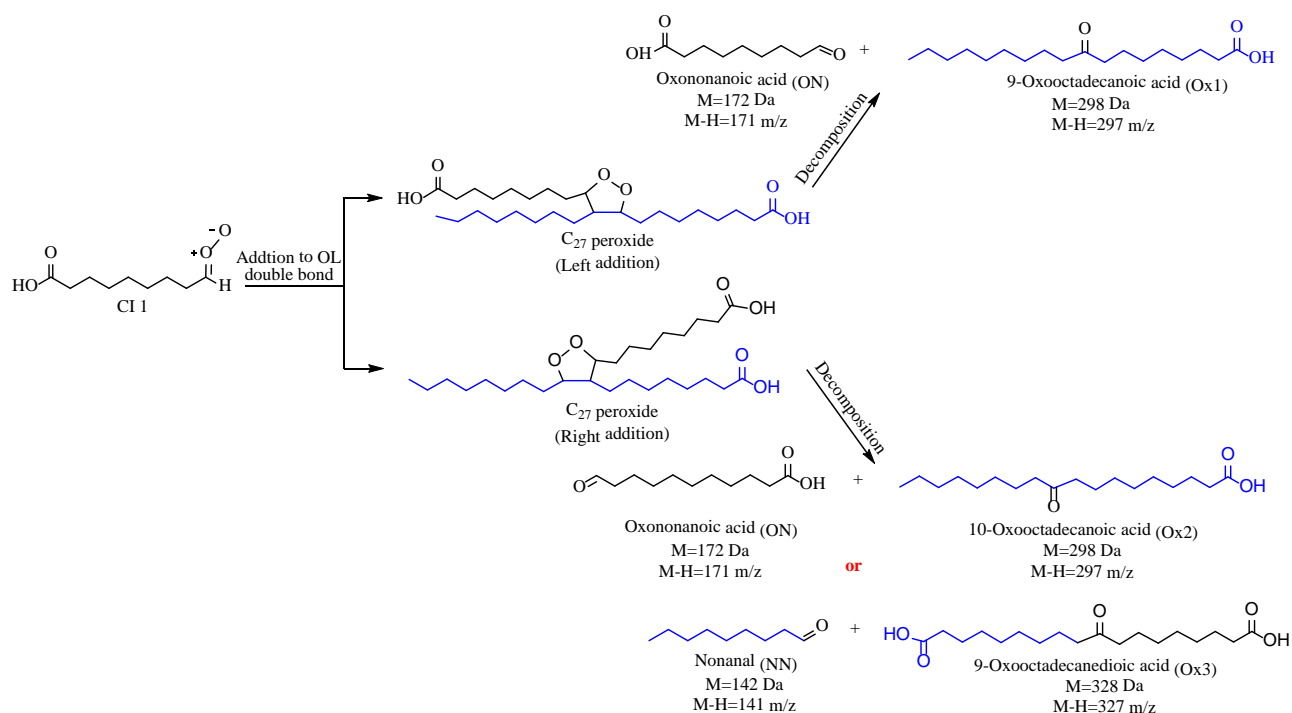
Scheme 2: Potential mechanism and product structures formed as a result of the reaction between CI1 and the alkene functionality of OL.

The existence of the carboxylic acid functionality in the oxidation products offers reaction sites for other CIs. The measured negative ion peaks at m/z -1019, -1189, and -1207 provide more evidence of the incorporation of Ox1 or Ox2 as linear polymerization propagators. However, the ion peak measured at m/z -644 is consistent with the formation of the ozonolysis product resulted from the reaction of two ions of CI1 and the two carboxylic moiety of one molecule of Ox.

The addition of CI2 terminates the polymerization reaction as the –CH$_3$ group cannot react further (Hung et al., 2005). The major HMW products ions at m/z -1025, -1079, -1214, -1292, -1310, -1346, -1438, and -1524 may also correspond to polymerization products of Ox3 joined with other propagators. Products related to the secondary reaction of ON are also observed in a number of peaks. The negative ion at m/z -341 is most likely due to the

combination of ON and CI1 to form AAHP (azelaic acid hydroperoxide) with a loss of one

molecule of water. Although the same combination can lead to the formation of the SOZ, in

such an arrangement a water molecule cannot be lost. The in situ dehydration of AAHP was

first observed and described by Zahardis and co-workers (Zahardis et al., 2006). The resultant

proposed structure suggests possible additional moieties linking from molecule ends, the

aldehyde and carboxylic acid groups, thereby growing into a HMW linear polymer; Scheme 3

shows the overall reaction; although the intermediate association complexes are unlikely to

be detected in reality, with conversion to the M-H = 341 product and elimination of water

proceeding as a concerted reaction.
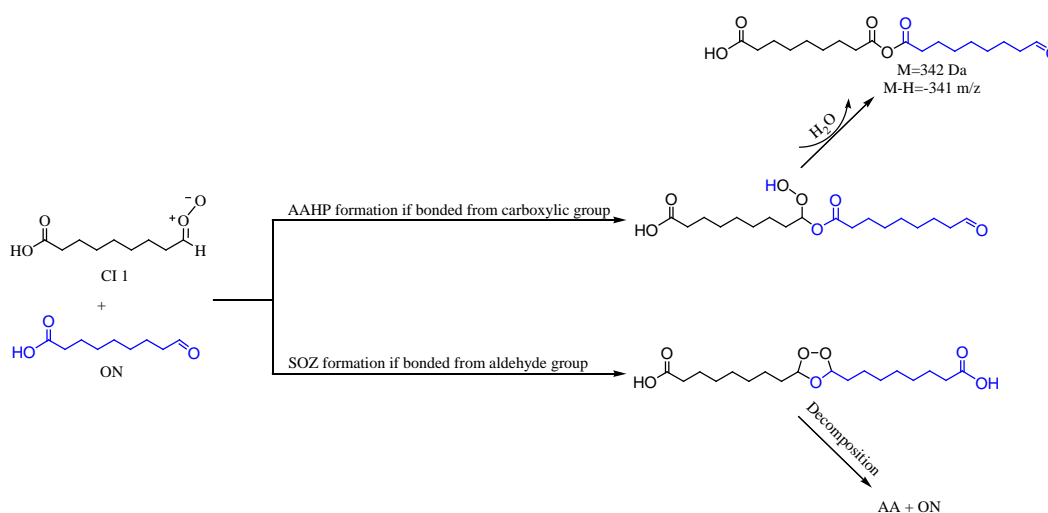
Scheme 3. Suggested reaction pathways and products of the secondary reaction between CI1 and ON.

3.8   Particle Composition as a Function of Particle Size

The ATOFMS technique allows for particle composition data to be collected as a function of

particle size, thereby permitting the size dependence of the chemical aging of aerosols to be

determined. This section investigates how the composition of aged OL particles changes,

under dry and humidified conditions, as a function of particle size. The analysis only

investigates the following compounds which have clear MS peaks: OL, NN, AA, ON, NA

and HMW compounds (m/z > 282). The conversion from measured peak area to molar

concentration is achieved using the standard calibration factor (SCF). Since an accurate SCF for the HMW compounds is difficult to determine due to the lack of standard laboratory calibrants, an upper limit value for the HMW SCF was estimated using a mass balance approach. In particular, the ratio between the OL signal to the total peak signals of the four primary oxidation products (AA, NN, NA and ON) was used to estimate the ratio between unreacted OL and the products. The obtained ratio of each product was corrected using the SCF to estimate the absolute molar ratio and hence the composition of the primary products in the particles. The reduction in the molar ratio between the four products and unreacted OL was used to estimate the SCF for the HMW (1 mole of OL produces 2 moles of the primary products (Scheme 1)).

3.9   Composition of Aged OL Particles Under Dry Conditions

Figure 7 provides the compositional analysis, by applying SCFs to the raw ATOFMS data, of 1000 aged OL particles that were ozonolysed under dry conditions. The size dependent composition is given in Figure 7a and the average composition of the aged OL polydisperse aerosol is shown in Figure 7b. The average composition was achieved by taking the mean of all mass fractions analysed regardless of size; since most particles were in the size range 0.3-0.5 µm this analysis will be biased towards this size fraction. The overall size distribution of the analysed particles was in the range 0.2-2.1 µm as measured by ATOFMS, see Figure 7c.

It can be clearly observed that the composition of aged particles is highly dependent on particle size. Firstly, larger particles contain more unreacted OL than smaller particles. This can be understood in terms of OL diffusivity within the particle and ozone flux into the particle. As the reaction progresses and oxidation products evolve at the reacted surface layer, both OL diffusivity within the particle and ozone diffusion to the bulk are reduced. Smith et

al. (2002) reported a low decay of OL in larger particles which was attributed by the limited OL diffusivity within the large particles. However, OL molecules in smaller particles (at a diameter size of 200 nm and less) are homogeneous in concentration and thus particles at this size and below are well mixed (Smith et al., 2002; Pfrang et al., 2010) facilitating the oxidation process and therefore the smaller the portion of unreacted OL. Additionally, in a simulation study, Shiraiwa et al. (2010) showed that ozone uptake drops upon reaction, attributed to a decrease in OL concentration at the particle surface (while it remains constant in the inner particle bulk, due to rapid bulk diffusion). It is therefore reasonable to conclude that the larger the particle the less the molar ratio of O_3:OL in the overall particle phase and hence the smaller the degree of oxidation and the greater proportion of unreacted OL. The fraction of NN in the particle tends to increase with particle size. The smallest size fraction contained only negligible amounts of NN. The vapour pressure of NN is 49.3 Pa at 25ºC (Daubert and Danner, 1989) and hence it is a highly volatile species which tends to partition to the vapour phase. In previous studies NN has been identified as one of the major volatile products (Moise and Rudich, 2002; Thornberry and Abbatt, 2004; Zahardis and Petrucci, 2007; Vesna et al., 2009; Dennis-Smither et al., 2012b), while few investigators detected NN in the particle phase using supermicron (King et al., 2004) and supported millimetre sized particles (Hung and Ariya, 2007). It is likely that NN has a low condensed phase yield in small particles due to its volatility that results in fast partition to the vapour phase. NN signals, however, were frequently enhanced in large particle spectra since its concentration in these particles was evolved from the secondary reaction within the particles, and products in these particles might reduce the effective vapour pressure of NN. Loss as vapour would also require diffusion within the condensed phase, which takes longer to reach the surface in the larger particles. Wang et al. have argued that all observed NN in the particle phase was

formed via secondary reactions though the study was conduct on pure OL particles of ~100 nm (Wang et al., 2016).

The mole fraction of AA, which arises from the rearrangement of CI1, was significantly larger in small particles compared to larger particles. It diminished appreciably in the most reacted larger particles suggesting the involvement of AA in the secondary chemistry associated more with larger particles. NA which arises from CI2 showed different trend to AA, and was not detected in small particles but observed in comparable fractions in larger size bins. This may reflect the volatile nature of NA which would reduce its impact in secondary chemistry as it tends to partition away from the particle. The steady decrease in ON mole fraction as particle size increases possibly indicates the involvement of ON in the secondary reactions associated with larger particles.

Figure 7a suggests that reactions in larger particles can appreciably enhance the formation of HMW (> 282 m/z) products. The chemical composition of larger particles, compared to smaller particles, is characterised by more unreacted OL, increased HMW products and less AA and ON. The low concentration of OL in small particles, however, minimizes these secondary pathways and maximizes the formation of the SOZ which subsequently dissociates to form the four primary oxidation products. The quantification analysis of processed OL particles by Katrib and co-workers showed no trend for AA with increasing OL layer thickness (2-30 nm), but high ON yield as compared to AA and NA yields was observed (Katrib et al., 2004), very consistent with our findings. They attributed their finding to the reactivity of the AA and NA precursors, i.e. CIs, being scavenged by OL. The presence of HMW products likely leads to greater aerosol viscosity and hence lower diffusion rates within the particle (Hosny et al., 2016). Hence larger particles will likely have slower diffusion rates which may in part explain the greater proportion of NN in the larger particles.

Moreover, measured viscosity of chemically aged aerosol might therefore be expected to vary substantially with - increase with - particle size, of relevance to the interpretation of aerosol particle viscosity measurements performed on individual super-micron samples.

3.10 Composition of Aged OL Particles under Wet Conditions

Figure 8 provides the corresponding compositional analysis, by applying SCFs to the raw ATOFMS data, of 1000 aged OL particles that were ozonolysed under humidified conditions. Significant differences in both the size dependent and average distribution of components between the dry and humidified oxidation runs were observed.

The greatest differences between the dry and wet oxidation data, averaged over all size bins for the complete polydisperse aerosol ensemble, is the reduction in HMW products from 13.0% under dry conditions compared to 4.5% under humidified conditions. The proportion of unreacted OL increases under humidified conditions (29.7%) compared to dry conditions (25.3%). Whilst OL is negligibly hygroscopic, ozonolysed OL is slightly hygroscopic (Lee et al., 2012). This slight hygroscopicity suggests that particle phase water could act as a reactant. The differences in composition between the dry and the humidified experiments could be explained by the preferential reactivity of CIs with water molecules compared to OL thereby resulting in a lower OL consumption under wet conditions. This chemistry results in less destruction of additional OL molecules via the secondary pathways, and hence the higher portion of unreacted OL and the limited amount of HMW products which are observed concomitantly under wetter conditions. The size distribution data from the SMPS, which indicated less mass loss during the humidified oxidation, supports this argument. AA in small particle sizes showed a significant change in these experiments. The observed amount of AA in the smallest particles (300 nm) increased under humid condition (Figure 8 and 7). This

result is partially supported by the study of Vesna et al. (2009), who used smaller particles (geometric mean diameter of 78 nm), and reported a similar trend with the smallest size bin of the particles in this study. The increase in the AA portion observed in response to the increase in the RH is consistent with our findings and it is attributed to water interference in supressing secondary reaction of AA with CIs, although Vesna et al. (2009) report a higher abundance of "unidentified products".

3.11 Kinetics of Oleic acid ozonolysis and product formation

The kinetics of the ozonolysis of a near-monodisperse sized ensemble of oleic acid particles in the size range of 0.4-0.5 μm with a mean diameter of 0.48 μm was investigated. Through the use of 3 different sized aerosol flow tubes (AFT), but with otherwise identical conditions to the experimental setup detailed previously, the interaction time between ozone and oleic acid particles could be obtained at 20, 50 and 135 s. The longest time was the same as that used in the product distribution study shown in Figures 7 and 8. In the absence of O_3 the effective interaction time is zero. We observed that the concentration of oleic acid was negligible at the longest interaction time (135 s) and hence the kinetics could only be followed in the time range of 0-50 s. The kinetics of the loss of OL was measured under both dry (0.5% RH) and humidified (65% RH) conditions. No significant difference was observed in dry and wet kinetics which is expected since oleic acid is only marginally hygroscopic and any water that is available will likely partition to the hygroscopic region of the molecule around the carboxylic acid functional group and not the lipophilic C=C double bond where the ozonolysis occurs.   Since the wet and dry runs were very similar, data from both runs were combined into a single dataset to increase the data points available for analysis. The measured data show a linear relationship between the plot of $\ln\{S(OL)/S(OL_0)\}$ versus interaction time, where S(OL) is the oleic acid signal, as shown in figure 9 below. This is consistent with surface limited reaction, as described by Case 3 kinetics initially proposed by Hearn et al. (2005). Using the same approach as Hearn et al. (2005), using the Case 3 kinetics approach, to derive gamma uptake coefficients (γ), we

obtain $\gamma = 5.6\pm0.2 \times 10^{-4}$ which is similar to previous measurements of γ, e.g. Hearn and Smith (2004), Moise and Rudich (2002), Hearn et al (2005), Thornberry and Abbatt (2004), Ziemann (2005), Knopf et al. (2005).

In addition to the oleic acid reactive decay kinetics, we also observed the time dependent formation of the four major first generation reaction products nonanoic acid (NA), azelaic acid (AA), nonanal (NN) and oxononanoic acid (ON), see Figure 10. The high molecular weight (HMW) products were not observable in these experimental runs which is consistent with the low levels observed in figures 7 and 8 in the 0.3-0.5 μm size bin. It is noted that low levels of HMW products were observed in the product distribution study but longer averaging times were used. It is clear that whilst the kinetics of oleic acid loss is very similar under both dry and humidified conditions, there are obvious differences in the formation kinetics of the four major first generation reaction products. In particular, under dry conditions the reaction products form more promptly, and once formed stay at relatively similar concentrations. Under humidified conditions the formation of the peak concentration of the products is slower but also their subsequent loss is more substantial. The kinetic data does not provide any definitive mechanistic understanding. However, these results are consistent with the hypothesis that water can act as a reactant with the CI thereby reducing the amount of secondary chemistry observed between OL and the primary reaction products, hence the more stable product distribution after the initial ozonolysis step.

3.11   Implications for Ageing Atmospheric Organic Aerosol

The observed reactions could have consequences for the ability of OL-derived particles (and OA of comparable functionality) to act as cloud condensation nuclei (CCN). Hygroscopicity greatly enhances the ability of particles to act as CCN, and consequently, oxidised particles containing a larger proportion of shorter-chain polar molecules are likely to be the most effective CCN for a given

particle size. King et al. (2009) use Köhler theory to demonstrate that the more oxidised particles will activate at a lower supersaturation than unreacted OL particles. However, the reduction in particle size which accompanies the loss of NN to the vapour phase will work in the opposite sense of increasing the critical supersaturation due to an increased Kelvin effect, at least for the smaller particles. However, since particles in the atmosphere are typically mixed and hence unlikely to comprise purely OL, even when emitted, such a discussion is likely to be of very limited relevance to atmospheric behaviour.

Heterogeneous reactions of organic particles directly alter the size, density and chemical composition of the particles. These are the key parameters controlling the particle's lifetime in the atmosphere and optical properties. While the size of the particle has considerable impact on the deposition velocity, wet scavenging efficiency and scattering of light, the identity of the species within the particle is the principal characteristic driving light absorption. The aging of organic aerosol can result in the formation of light absorbing species. The large numbers of organic functionalities in SOA such as carboxylate, hydroxyl, ketone and aldehyde groups may result in an absorbing matrix that can exhibit optical properties dramatically different from those of parent molecules. Particles containing light absorbers may lead to heating of the lower atmosphere resulting in positive global radiative forcing. The impact of SOA on global radiative forcing is thus one of the largest uncertainties in atmospheric science. On the other hand, the presence of absorbing compounds in organic particles can stimulate photosensitization processes which might lead to either reduction and oxidation of intermediates and products (Kolb et al., 2010). For the reasons outlined above, because of the internally mixed nature of airborne particles, closer examination of the properties of oxidised OL particles is unlikely to be of major relevance to prediction of the properties of atmospheric aerosol.

4.   CONCLUSION

This study demonstrates a link between the particle size and reaction mechanisms within OL aerosol. Aged finer particles are likely to be more hydrophilic due to the oxidation of the OL in the particles and the formation of an early generation of more polar, and hence more hygroscopic oxidation products. However, the combination of unreacted OL, HMW products and volatile product observed in large particles suggests overall hydrophobicity of larger particles. The difference in the reactivity of OL at different relative humidities with less OL destruction observed under humid conditions can be explained by the preference of CIs for reaction with water molecules over the reaction with OL, which results in less oligomerisation.

There has been some speculation in the literature as to the effects of oxidation upon atmospherically relevant properties of OL particles, such as their ability to act as CCN. However, the relevance of extrapolation to the atmospheric context, except in a generic sense, is extremely limited due to the complex internal mixing of atmospheric particles, even when emitted, and hence the extreme improbability of pure OL particles existing in the atmosphere. However, in our view, the value of studies such as this is in the enhanced mechanistic understanding gained from treating OL oxidation by ozone as a model system. In particular, there is limited understanding of processes leading to the formation of highly functionalised oxidised high molecular weight products, such as those observed in this work.

REFERENCES

Allen, J. O.: Quantitative analysis of aerosol time-of-flight mass spectrometry data using YAADA. Arizona States, Arizona State University, 65, 2004.

Allen, J. O., Bhave, P. V., Whiteaker, J. R. and Prather, K. A.: Instrument busy time and mass measurement using aerosol time-of-flight mass spectrometry, Aerosol Sci. and Technol., 40, 615-626, 2006.

Andrews, E. and Larson, S. M.: Effect of surfactant layers on the size changes of aerosol particles as a function of relative humidity, Environ. Sci. Technol., 27, 857-865, 1993.

Bhave, P. V., Allen, J. O., Morrical, B. D., Fergenson, D. P., Cass, G. R. and Prather, K. A.: A field-based approach for determining ATOFMS instrument sensitivities to ammonium and nitrate, Environ. Sci.Technol., 36, 4868-4879, 2002.

Carlton, A. G., Pinder, R. W., Bhave, P. V. and Pouliot, G. A.: To what extent can biogenic SOA be controlled?, Environ. Sci. Technol., 44, 3376-3380, 2010.

Chan, M. N., Nah, T. and Wilson, K. R.: Real time in situ chemical characterization of sub-micron organic aerosols using Direct Analysis in Real Time mass spectrometry (DART-MS): the effect of aerosol size and volatility, Analyst, 138, 3749-3757, 2013.

Dall'Osto, M., Harrison, R. M., Beddows, D. C., Freney, E. J., Heal, M. R. and Donovan, R. J.: Single-particle detection efficiencies of aerosol time-of-flight mass spectrometry during the North Atlantic marine boundary layer experiment, Environ. Sci. Technol., 40, 5029-5035, 2006.

Dall'Osto, M. and Harrison, R. M.: Urban organic aerosols measured by single particle mass spectrometry in the megacity of London, Atmos. Chem. Phys., 12, 4127-4142, 2012.

Daubert, T. E. and Danner R. P.: Physical and thermodynamic properties of pure chemicals: Data compilation, Taylor & Francis, 1989.

Dennis-Smither, B. J., Hanford, K. L., Kwamena, N.-O. A., Miles, R. E. H. and Reid, J. P.: Phase, morphology, and hygroscopicity of mixed oleic acid/sodium chloride/water aerosol particles before and after ozonolysis, J. Phys. Chem. A, 116, 6159-6168, 2012a.

Dennis-Smither, B. J., Miles, R. E. H. and Reid, J. P.: Oxidative aging of mixed oleic acid/sodium chloride aerosol particles, J. Geophys. Res.: Atmospheres, 117(D20), D20204, doi 10.1029/2012JD018163, 2012b.

Fergenson, D. P., Song, X.-H., Ramadan, Z., Allen, J. O., Hughes, L. S., Cass, G. R., Hopke, P. K. and Prather, K. A.: Quantification of ATOFMS data by multivariate methods, Anal. Chem., 73, 3535-3541, 2001.

Finlayson-Pitts, B. J. and Pitts Jr, J. N.: Analytical methods and typical atmospheric concentrations for gases and particles. Chemistry of the upper and lower atmosphere, Chapter 11, 547-656, Academic Press, San Diego, 2000.

Gallimore, P. J., Achakulwisut, P., Pope, F. D., Davies, J. F., Spring, D. R. and Kalberer, M.: Importance of relative humidity in the oxidative ageing of organic aerosols: case study of the ozonolysis of maleic acid aerosol, Atmos. Chem. Phys., 11, 12181-12195, 2011.

Gard, E., Mayer, J. E., Morrical, B. D., Dienes, T., Fergenson, D. P. and Prather, K. A.: Real-time analysis of individual atmospheric aerosol particles: Design and performance of a portable ATOFMS, Anal. Chem., 69, 4083-4091, 1997.

Gard, E. E., Kleeman, M. J., Gross, D. S., Hughes, L. S., Allen, J. O., Morrical, B. D., Fergenson, D. P., Dienes, T., Gälli, M. E., Johnson, R. J., Cass, G. R. and Prather, K. A.: Direct observation of heterogeneous chemistry in the atmosphere, Science, 279, 1184-1187, 1998.

Goldstein, A. H., Galbally, I. E.: Known and unexplored organic constituents in the Earth's atmosphere, Environ. Sci. Technol., 41, 1515-1521, 2007.

Gonzalez-Labrada, E., Schmidt, R. and DeWolf, C. E.: Kinetic analysis of the ozone processing of an unsaturated organic monolayer as a model of an aerosol surface, Phys.Chem. Chem. Phys., 9, 5814-5821, 2007.

Grimm, R. L., Hodyss, R. and Beauchamp, J. L.: Probing interfacial chemistry of single droplets with field-induced droplet ionization mass spectrometry: Physical adsorption of polycyclic aromatic hydrocarbons and ozonolysis of oleic acid and related compounds, Anal. Chem., 78, 3800-3806, 2006.

Gross, D. S., Galli, M. E., Silva, P. J., Wood, S. H., Liu, D.-Y. and Prather, K. A.: Single particle characterization of automobile and diesel truck emissions in the Caldecott Tunnel, Aerosol Sci. Technol., 32, 152-163, 2000.

Harrison, R. M.: Pollution: Causes, Effects and Control, Fifth Edition, Royal Society of Chemistry, Cambridge, 2014.

Hearn, J. D. and Smith, G. D.: Kinetics and product studies for ozonolysis reactions of organic particles using aerosol CIMS†, J. Phys. Chem. A, 108, 10019-10029, 2004.

Hearn, J. D., Lovett, A. J. and Smith, G. D.: Ozonolysis of oleic acid particles: evidence for a surface reaction and secondary reactions involving Criegee intermediates, Phys. Chem. Chem. Phys., 7, 501-511, 2005.

Hosny, N. A., Fitzgerald, C., Tong, C., Kalberer, M., Kuimova, M. K. and Pope, F. D.: Fluorescent lifetime imaging of atmospheric aerosols: a direct probe of aerosol viscosity, Faraday Discuss., 165, 343-356, 2013.

Hosny, N. A., Fitzgerald, C., Vyšniauskas, A., Athanasiadis, A., Berkemeier, T., Uygur, N., Pöschl, U., Shiraiwa, M., Kalberer, M., Pope, F. and Kuimova, M. K.: Direct imaging of changes in aerosol particle viscosity upon hydration and chemical aging, Chem. Sci., 2041-6520, 2016.

Hung, H.-M., Katrib, Y. and Martin, S. T.: Products and mechanisms of the reaction of oleic acid with ozone and nitrate radical, J. Phys.Chem. A, 109, 4517-4530, 2005.

Hung, H.-M. and Ariya, P.: Oxidation of oleic acid and oleic acid/sodium chloride(aq) mixture droplets with ozone: Changes of hygroscopicity and role of secondary reactions, J. Phys. Chem. A, 111, 620-632, 2007.

Hung, H.-M. and Tang, C.-W.: Effects of temperature and physical state on heterogeneous oxidation of oleic acid droplets with ozone, J. Phys. Chem. A, 114, 13104-13112, 2010.

Katrib, Y., Martin, S. T., Hung, H.-M., Rudich, Y., Zhang, H., Slowik, J. G., Davidovits, P., Jayne, J. T. and Worsnop, D. R.: Products and mechanisms of ozone reactions with oleic acid for aerosol particles having core–shell morphologies, J. Phys. Chem. A, 108, 6686-6695, 2004.

Katrib, Y., Biskos, G., Buseck, P. R., Davidovits, P., Jayne, J. T., Mochida, M., Wise, M. E., Worsnop, D. R. and Martin, S. T.: Ozonolysis of mixed oleic-acid/stearic-acid particles: Reaction kinetics and chemical morphology, J. Phys. Chem. A, 109, 10910-10919, 2005a.

Katrib, Y., Martin, S. T., Rudich, Y., Davidovits, P., Jayne, J. T. and Worsnop, D. R.: Density changes of aerosol particles as a result of chemical reaction, Atmos. Chem. Phys., 5, 275-291, 2005b.

King, M. D., Thompson, K. C. and Ward, A. D.: Laser Tweezers raman study of optically trapped aerosol droplets of seawater and oleic acid reacting with ozone: Implications for cloud-droplet properties, J. Am. Chem. Soc., 126, 16710-16711, 2004.

King, M. D., Rennie, A. R., Thompson, K. C., Fisher, F. N., Dong, C. C., Thomas, R. K., Pfrang, C. and Hughes, A. V.: Oxidation of oleic acid at the air-water interface and its potential effects on cloud critical supersaturations, Phys. Chem. Chem.Phys., 11, 7699-7707, 2009.

Kolb, C., Cox, R., Abbatt, J., Ammann, M., Davis, E., Donaldson, D., Garrett, B. C., George, C., Griffiths, P. and Hanson, D.: An overview of current issues in the uptake of atmospheric trace gases by aerosols and clouds, Atmos.Chem. Phys., 10, 10561-10605, 2010.

Kolb, C. E. and Worsnop D. R.: Chemistry and composition of atmospheric aerosol particles, Annual Rev. Phys.Chem., 63, 471-491, 2012.

Koop, T., Bookhold, J., Shiraiwa, M. and Pöschl, U.: Glass transition and phase state of organic compounds: dependency on molecular properties and implications for secondary organic aerosols in the atmosphere, Phys. Chem. Chem. Phys., 13, 19238-19255, 2011.

Kroll, J. H. and Seinfeld, J. H.: Chemistry of secondary organic aerosol: Formation and evolution of low-volatility organics in the atmosphere, Atmos. Environ., 42, 3593-3624, 2008.

Kumar, P., Broekhuizen, K. and Abbatt, J. P. D.: Organic acids as cloud condensation nuclei: Laboratory studies of highly soluble and insoluble species, Atmos. Chem. Phys., 3, 509-520, 2003.

Lee, A. K. Y. and Chan, C. K.: Single particle Raman spectroscopy for investigating atmospheric heterogeneous reactions of organic aerosols, Atmos. Environ., 41, 4611-4621, 2007.

Lee, J. W. L., Carrascon, V., Gallimore, P. J., Fuller, S. J., Bjorkegren, A., Spring, D. R., Pope ,F. D. and Kalberer, M.: The effect of humidity on the ozonolysis of unsaturated compounds in aerosol particles, Phys.Chem. Chem. Phys., 14, 8023-8031, 2012.

Mendez, M., Visez, N., Gosselin, S., Crenn, V., Riffault, V. and Petitprez, D.: Reactive and Nonreactive Ozone Uptake during Aging of Oleic Acid Particles, J. Phys.Chem. A, 118, 9471-9481, 2014.

Moise, T. and Rudich, Y.: Reactive uptake of ozone by aerosol-associated unsaturated fatty acids: Kinetics, Mechanism, and products, J. Phys. Chem. A, 106, 6469-6476, 2002.

Morris, J. W., Davidovits, P., Jayne, J. T., Jimenez, J. L., Shi, Q., Kolb, C. E., Worsnop, D. R., Barney, W. S. and Cass, G.: Kinetics of submicron oleic acid aerosols with ozone: A novel aerosol mass spectrometric technique, Geophys. Res. Lett., 29, No. 9, 1357, doi 10.1029/2002GL014692, 2002.

Nash, D. G., Baer, T. and Johnston, M. V.: Aerosol mass spectrometry: An introductory review, Intl J. Mass Spectrom., 258, 2-12, 2006.

Neeb, P., Horie, O. and Moortgat, G. K.: The ethene–ozone reaction in the gas phase, J. Phys. Chem. A, 102, 6778-6785, 1998.

Park, J., Gomez, A. L., Walser, M. L., Lin, A. and Nizkorodov, S. A.: Ozonolysis and photolysis of alkene-terminated self-assembled monolayers on quartz nanoparticles: implications for photochemical aging of organic aerosol particles, Phys. Chem. Chem. Phys., 8, 2506-2512, 2006.

Park, S. S., Kim, J.-H. and Jeong, J.-U.: Abundance and sources of hydrophilic and hydrophobic water-soluble organic carbon at an urban site in Korea in summer, J. Environ. Monit., 14, 224-232 2012.

Petters, M. D., Prenni, A. J., Kreidenweis, S. M., DeMott, P. J., Matsunaga, A., Lim, Y. B. and Ziemann, P. J.: Chemical aging and the hydrophobic-to-hydrophilic conversion of carbonaceous aerosol, Geophys. Res. Lett., 33, L24806, doi 10.1029/2006GL027249, 2006.

Pfrang, C., Shiraiwa, M. and Pöschl, U.: Coupling aerosol surface and bulk chemistry with a kinetic double layer model (K2-SUB): oxidation of oleic acid by ozone, Atmos. Chem. Phys., 10, 4537-4557, 2010.

Pöschl, U.: Gas-particle interactions of tropospheric aerosols: Kinetic and thermodynamic perspectives of multiphase chemical reactions, amorphous organic substances, and the activation of cloud condensation nuclei, Atmos. Res., 562-573, 2011.

Reynolds, J. C., Last, D. J., McGillen, M., Nijs, A., Horn, A. B., Percival, C., Carpenter, L. J. and Lewis, A. C.: Structural analysis of oligomeric molecules formed from the reaction products of oleic acid ozonolysis, Environ. Sci. Technol., 40, 6674-6681, 2006.

Rudich, Y.: Laboratory perspectives on the chemical transformations of organic matter in atmospheric particles, Chem. Rev., 103, 5097-5124, 2003.

Shiraiwa, M., Pfrang, C. and Pöschl, U.: Kinetic multi-layer model of aerosol surface and bulk chemistry (KM-SUB): the influence of interfacial transport and bulk diffusion on the oxidation of oleic acid by ozone, Atmos. Chem. Phys., 10, 3673-3691, 2010.

Silva, P. J. and Prather, K. A.: Interpretation of mass spectra from organic compounds in aerosol time-of-flight mass spectrometry, Anal. Chem., 72, 3553-3562, 2000.

Smith, G. D., Woods, E., DeForest, C. L., Baer, T. and Miller, R. E.: Reactive uptake of ozone by oleic acid aerosol particles: Application of single-particle mass spectrometry to heterogeneous reaction kinetics, J. Phys. Chem. A, 106, 8085-8095, 2002.

Sullivan, R. C. and Prather, K. A.: Recent advances in our understanding of atmospheric chemistry and climate made possible by on-line aerosol analysis instrumentation, Anal. Chem., 77, 3861-3886, 2005.

Thornberry, T. and Abbatt, J. P. D.: Heterogeneous reaction of ozone with liquid unsaturated fatty acids: detailed kinetics and gas-phase product studies, Phys.Chem. Chem. Phys., 6, 84-93, 2004.

Vesna, O., Sjogren, S., Weingartner, E., Samburova, V., Kalberer, M., Gäggeler, H. W. and Ammann, M.: Changes of fatty acid aerosol hygroscopicity induced by ozonolysis under humid conditions, Atmos. Chem. Phys., 8, 4683-4690, 2008.

Vesna, O., Sax, M., Kalberer, M., Gaschen, A. and Ammann, M.: Product study of oleic acid ozonolysis as function of humidity, Atmos. Environ., 43, 3662-3669, 2009.

von Hessberg, C., von Hessberg, P., Pöschl, U., Bilde, M., Nielsen, O. J. and Moortgat G. K.:Temperature and humidity dependence of secondary organic aerosol yield from the ozonolysis of β-pinene, Atmos. Chem. Phys., 9, 3583-3599, 2009.

Wang, M., Yao, L., Zheng, J., Wang, X., Chen, J., Yang, X., Worsnop, D. R., Donahue, N. M. and Wang, L.: Reactions of atmospheric particulate stabilized Criegee intermediates lead to high-molecular-weight aerosol components, Environmental science & technology, 50, 5702ental s2016.

Zahardis, J., LaFranchi, B. W. and Petrucci, G. A.: Photoelectron resonance capture ionization-aerosol mass spectrometry of the ozonolysis products of oleic acid particles: Direct measure of higher molecular weight oxygenates, J. Geophys. Res.: Atmospheres, 110(D8), D08307, doi 10.1029/2004JD005336, 2005.

Zahardis, J., LaFranchi, B. W. and Petrucci, G. A.: Direct observation of polymerization in the oleic acid–ozone heterogeneous reaction system by photoelectron resonance capture ionization aerosol mass spectrometry, Atmos. Environ., 40, 1661-1670, 2006.

Zahardis, J. and Petrucci, G. A.: The oleic acid-ozone heterogeneous reaction system: products, kinetics, secondary chemistry, and atmospheric implications of a model system; a review, Atmos. Chem. Phys., 7, 1237-1274, 2007.

Ziemann, P. J.: Aerosol products, mechanisms, and kinetics of heterogeneous reactions of ozone with oleic acid in pure and mixed particles, Faraday Discuss., 130, 469-490, 2005.

TABLE LEGENDS

Table 1:   A summary of proposed components and possible propagator combinations contributing to of observed mass spectral peaks corresponding to 44 oxidation products of the OL-O_3 system.

FIGURE LEGENDS

Figure 1:   The experimental setup for the study of the heterogeneous oxidation of OL aerosol.

Figure 2:   Particle mass size distributions for (a) pure and oxidised OL aerosol under dry condition (RH $0.5 \pm 0.02\%$), (b) pure and oxidised OL aerosol under wet condition (RH $65.0 \pm 0.2\%$) and (c) normalised particle size distribution of pure and oxidised OL aerosol under dry and wet conditions. Each curve represents the mean average of 10 measurements with accompanying standard deviation (σ).

Figure 3:   Positive and negative ion mass spectra of OL, AA, NA, NN and 4-ON. Each spectrum presented represents the average from 100 mass spectra.

Figure 4:   Relative peak area signals from aerosol particles generated from an eqimolar mixture of OL, AA, NA, NN and 4-ON. Peak areas are an average from 200 mass spectra.

Figure 5:   Averaged ATOFMS negative and positive ion mass spectra for small processed OL particles (Dp < 0.3 µm).

Figure 6:   Average mass spectra of dry aged OL particles (Dp>0.3 µm): (a) negative ion MS (b) zoom in plot of figure (a) and (c) positive ion MS.

Figure 7:   ATOFMS data analysis of: (a) mole fraction of ozonolysed OL particles, under dry conditions, as a function of particle size, (b) total particle composition as given by mole fraction for all size fractions, and (c) Corresponding size distribution of the aged OL aerosol measured by ATOFMS.

Figure 8:   ATOFMS data analysis of: (a) mole fraction of ozonolysed OL particles, under humidified conditions, as a function of particle size, (b) total particle composition as given by mole fraction for all size fractions, and (c) corresponding size distribution of the aged OL aerosol measured by ATOFMS.

Table 1: A summary of proposed components and possible propagator combinations contributing to of observed mass spectral peaks corresponding to 44 oxidation products of the OL-O$_3$ system

	MS signature		No of composed components								
MW	- m/z	+ m/z	NN	OcA	AA or CI1	ON	NA or CI2	Ox1 or Ox2	Ox3	OL	Dehydration (-nH$_2$O)
142	141		1								
144	143			1							
158	157						1				
170	169				1						1
172	171					1					
188	187				1						
298	297							1			
314	313			1	1						
328	327							1			
342	341				1	1					
422	421	377*					1			1	1
440	439	423†					1			1	0
528	527	466*† 483* 547‡			3						3
644	643	599*					2	1			0
656	655				2		2				2
768	767				1		2		1		1
786	785	753#			1		2		1		0
810	809	793† 777#			2	1	2				3
844	843	811#			3		2				2
864	863	819* 831#			2	1	2				0
880	879				3		2				0
894	893	861#			3	1	1				0
950	949	917#			3		1		1		3
968	967	935#			3		1		1		2
974	973				2		2		1		0
986	985	953#			3		1		1		1

1002	1001				3		3				2
1020	1019	1003†			3		1	1			0
1026	1025				4				1		3
1038	1037	1005⁎			3		3				0
1051	1050	1070‡			4		2				1
1068	1067	1023* 1106‡			4		2				0
1080	1079				4				1		0
1162	1161	1112†⁎			3		2			1	0
1178	1177				3		4				1
1190	1189				4		1	1			1
1196	1195				3		4				0
1208	1207				4		1	1			0
1214	1213				5				1		3
1292	1291				3	1			1	1	3
1310	1309				3	1			1	1	2
1346	1345				3	1			1	1	0
1438	1437				6				1		1
1524		1458⁎			3		4		1		0

*M-CO$_2$H, ⁎M-HO$_2$, †M-OH and ‡M+H$_3$O.

Figure 1: The experimental setup for the study of the heterogeneous oxidation of OL aerosol

Figure 2: Particle mass size distributions for (a) pure and oxidised OL aerosol under dry condition (RH 0.5 ± 0.02%), (b) pure and oxidised OL aerosol under wet condition (RH 65.0 ± 0.2%) and (c) normalised particle size distribution of pure and oxidised OL aerosol under dry and wet conditions. Each curve represents the mean average of 10 measurements with accompanying standard deviation (σ)

Figure 3: Positive and negative ion mass spectra of OL, AA, NA, NN and 4-ON. Each spectrum presented represents the average from 100 mass spectra

Figure 4: Relative peak area signals from aerosol particles generated from an eqimolar mixture of OL, AA, NA, NN and 4-ON. Peak areas are an average from 200 mass spectra

Figure 5: Averaged ATOFMS negative and positive ion mass spectra for small processed OL particles (Dp < 0.3 μm)

Figure 6: Average mass spectra of dry aged OL particles (Dp>0.3 µm): (a) negative ion MS (b) zoom in plot of figure (a) and (c) positive ion MS

Figure 7: ATOFMS data analysis of: (a) mole fraction of ozonolysed OL particles, under dry conditions, as a function of particle size, (b) total particle composition as given by mole fraction for all size fractions, and (c) corresponding size distribution of the aged OL aerosol measured by ATOFMS
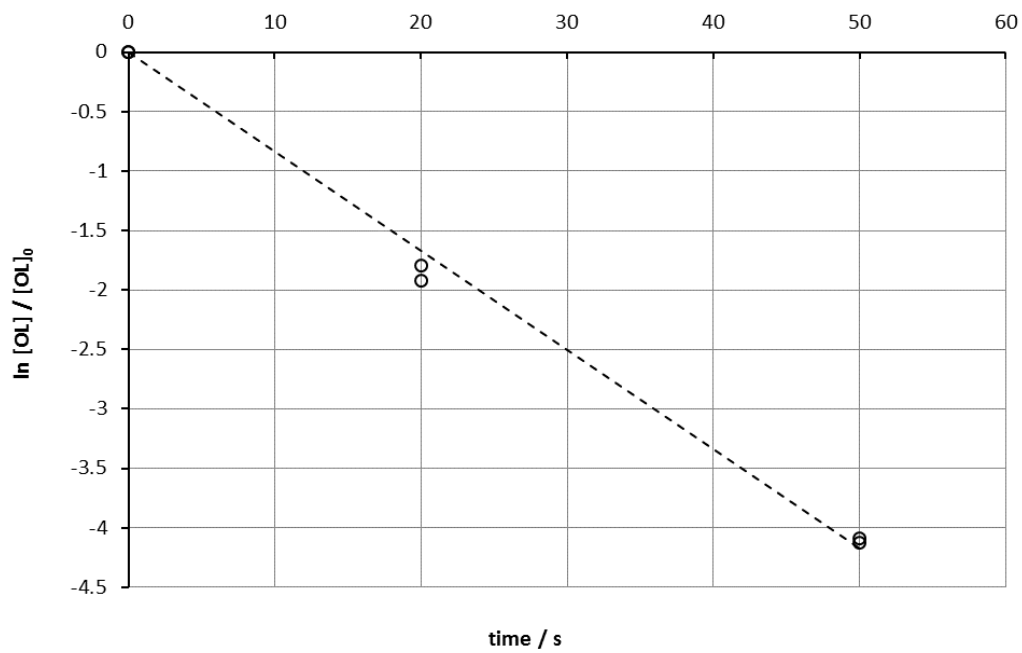
Figure 8: ATOFMS data analysis of: (a) mole fraction of ozonolysed OL particles, under humidified conditions, as a function of particle size, (b) total particle composition as given by mole fraction for all size fractions, and (c) corresponding size distribution of the aged OL aerosol measured by ATOFMS

Figure 9. Reactive decay of oleic acid as a function of time for particles in the size range 0.4-0.5 μm (mean diameter = 0.48 μm). Black circles = measurements, dashed line = linear fit with intercept set to zero. Both the dry and wet kinetic data has been combined in this plot.

SUPPORTING INFORMATION

SIZE DEPENDENT CHEMICAL AGEING OF OLEIC ACID AEROSOL

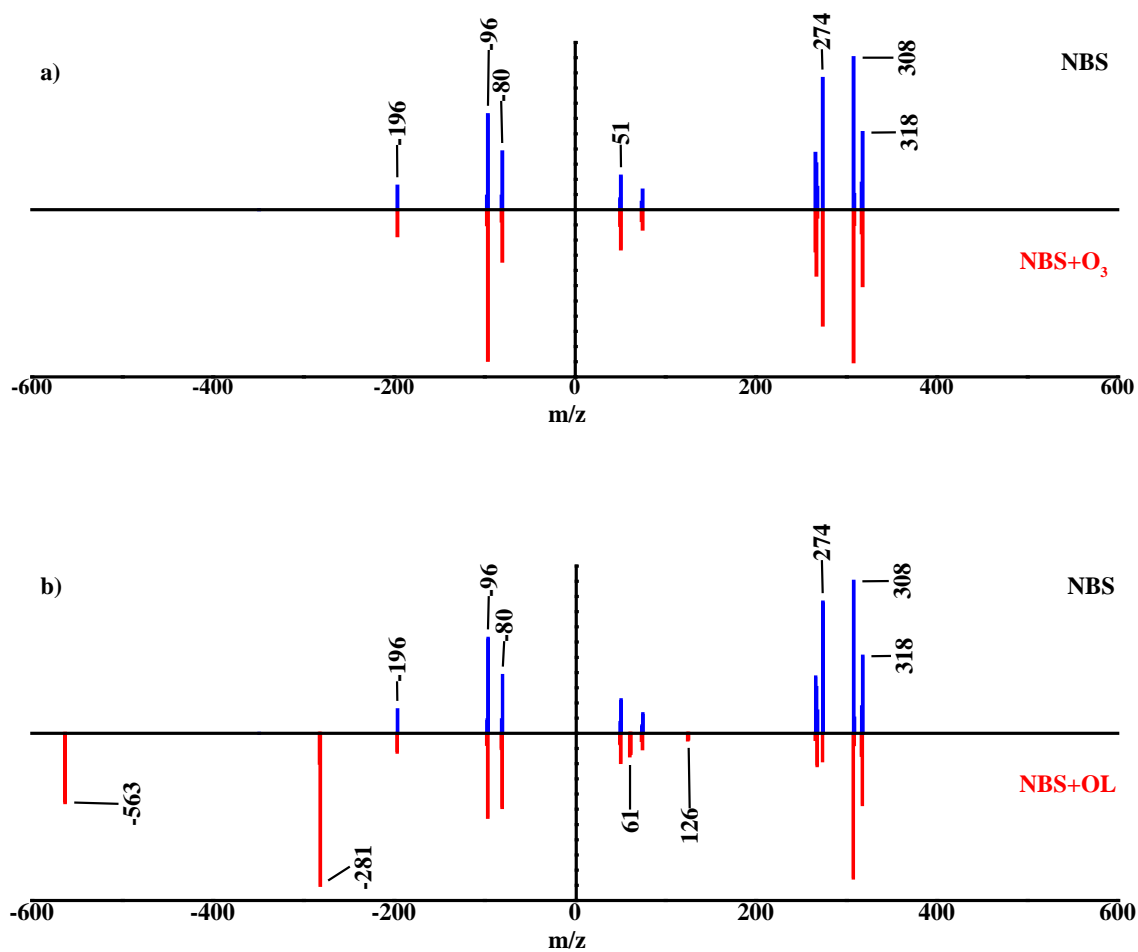**Suad S. Al-Kindi, Francis D. Pope, David C. Beddows, William J. Bloss and Roy M. Harrison**

Figure S1: Positive and negative mass spectra of (a) NBS and NBS exposed to O_3 and (b) NBS and OL in NBS solution. Each spectrum presented represents the averages from 100 spectra